# PETROGRAPHIC STUDY OF FOUR SAMPLES RECOVERED FROM THE NAHANNI FORMATION AT WELL LOCATION B.A. TEXACO ARROWHEAD N-02 300/N-02-6040-12300/0

**Northwest Territories Geological Survey**
**Work Order No. 20A20312**

**March, 2020**

**AGAT Laboratories**
3801 – 21st Street N.E.
Calgary, Alberta T2E 6T5

AGAT Laboratories

SERVICE BEYOND ANALYSIS

AGAT

# TABLE OF CONTENTS


Executive Summary . . . . . . . . . . . . . . . . . . . . . . . . . . . . . . . . . . . . . . . . . . . . . . . . . . . . . . . . .2

Methods of Analysis . . . . . . . . . . . . . . . . . . . . . . . . . . . . . . . . . . . . . . . . . . . . . . . . . . . . . 7

Abbreviations . . . . . . . . . . . . . . . . . . . . . . . . . . . . . . . . . . . . . . . . . . . . . . . . . . . . . . . . . 11

Results

Sample T25/S25 (10015.50ft/3052.72m). . . . . . . . . . . . . . . . . . . . . . . . . . . . . . . . . . . 12

Thin Section Analysis . . . . . . . . . . . . . . . . . . . . . . . . . . . . . . . . . . . . . . . . . . . . 14

SEM Analysis . . . . . . . . . . . . . . . . . . . . . . . . . . . . . . . . . . . . . . . . . . . . . . . . . .16

Sample T24/S24 (10020.00ft/3054.10m). . . . . . . . . . . . . . . . . . . . . . . . . . . . . . . . . . . 18

Thin Section Analysis . . . . . . . . . . . . . . . . . . . . . . . . . . . . . . . . . . . . . . . . . . . . 19

SEM Analysis . . . . . . . . . . . . . . . . . . . . . . . . . . . . . . . . . . . . . . . . . . . . . . . . . . 21

Sample T23/S23 (10023.75ft/3055.24m). . . . . . . . . . . . . . . . . . . . . . . . . . . . . . . . . . . 23

Thin Section Analysis . . . . . . . . . . . . . . . . . . . . . . . . . . . . . . . . . . . . . . . . . . . . 24

SEM Analysis . . . . . . . . . . . . . . . . . . . . . . . . . . . . . . . . . . . . . . . . . . . . . . . . . . 26

Sample T22/S22 (10042.20ft/3060.86m). . . . . . . . . . . . . . . . . . . . . . . . . . . . . . . . . . . 28

Thin Section Analysis . . . . . . . . . . . . . . . . . . . . . . . . . . . . . . . . . . . . . . . . . . . . 29

SEM Analysis . . . . . . . . . . . . . . . . . . . . . . . . . . . . . . . . . . . . . . . . . . . . . . . . . . 30

Summary of Pore System, Main Porosity Controls and Reservoir Quality . . . . . . . . 33

References . . . . . . . . . . . . . . . . . . . . . . . . . . . . . . . . . . . . . . . . . . . . . . . . . . . . . . . . . . . 37

Appendix/Data Tables

Table 1: Petrographic Summary - T 22 to T25

Table 2: Bulk XRD Data

## EXECUTIVE SUMMARY

The purpose of this study is to describe the observed lithological characteristics, associated reservoir quality and fluid sensitivity of four petrographic samples collected from the Nahanni Formation at well location B.A. TEXACO ARROWHEAD N-02 300/N-02-6040-12300/0. Petrographic analyses and interpretations are based on the observation of thin section and SEM samples generated from core. Other analyses that were completed on all four samples include Bulk XRD and Routine Core Analysis (RCA). RCA analysis (Work Order # RC31658) that include porosity, permeability, plus grain density of the core plug samples has been submitted to Northwest Territories Geological Survey at the end of February 2020. The RCA data (porosity and permeability) can also be seen in the Petrographic Summary **Table 1**. The Bulk XRD analysis are presented in **Table 2.** Both tables can be found in the Tables and Figures section of this report. An overview of general sample information that includes sample ID used for each types of the analysis, depth (ft & m), stratigraphic unit, rock classification, analysis performed, plus overall reservoir quality, can be found below within **Table A:**

| **Sample ID (*)** | **Depth (ft & m)** | **Formation** | **Rock Classification** | **Analysis (*)** | **RQ (*)** |
|---|---|---|---|---|---|
| **Location: B.A. Texaco Arrowhead N-02 300/N-02-6040-12300/0** | | | | | |
| T25/S25/X43/P15 | 10015.50ft 3052.72m | Nahanni | Dolostone (Mudstone) | TS; SEM; XRD; RCA | P |
| T24/S24/X42/P14 | 10020.00ft 3054.10m | Nahanni | Dolostone (Packstone-Wackestone) | TS; SEM; XRD; RCA | P |
| T23/S23/X41/P13 | 10023.75ft 3055.24m | Nahanni | Dolostone (Mudstone-Wackestone-Packstone) | TS; SEM; XRD; RCA | P |
| T22/S22/X40/P12 | 10042.20ft 3060.86m | Nahanni | Dolostone (Wackestone-Packstone) | TS; SEM; XRD; RCA | P |

**(*) Sample ID: T: thin section; S: SEM; X: XRD; P: core plug**

**(*) TS- Detailed thin section analysis with Images; XRD: Bulk & Clay X-Ray Analysis; RCA – Routine Core Analysis**

**(*) RQ (Reservoir Quality): VP – Very Poor; P- Poor; M – Moderate; G- Good**

All four samples recovered from the Nahanni Formation at the study location are dolostones. Based on the preserved original texture of the precursor sediment, the samples were classified as mudstone (T25), packstone to wackestone (T24), mudstone to wackestone and packstone (T23), plus wackestone to packstone (T22). The mineral composition is dominated by dolomite (68% to 96%), with lesser amounts of detrital quartz grains [15% in sample T23 and 30% in sample T25]. Additionally minor calcite (1% to 5%), trace to minor pyrite (trace to 1%), plus trace clays and organics (all samples), and trace rock fragments (only in sample T25) were detected during the thin section examination. The framework builders are represented by carbonate clasts and bioclast fragments. The carbonate clasts, which are totally dolomitized, occur as peloids [1% in sample T25, plus 20% to 35% in the other three samples], intraclasts (trace to 2% - except for sample T24), plus trace ooids (only in samples T25 and T23). Bioclasts were spotted in abundance in sample T24 (45%) and T22 (25%) and in minor amounts in sample T23 (2%). The quartz-rich dolo-mudstone (sample T25) does not contain any bioclast fragments. The bioclast fragments are represented by annelid worms (T24), mollusks and brachiopods, algae, ostracodes, corals, plus unidentified bioclast. The majority of bioclasts are replaced/cemented with dolomite and or calcite spar, but occasionally un-dolomitized (calcitic) coral fragments were also spotted during the thin section examination. Detrital quartz is locally incorporated into small lenses (sample T25) or it is randomly distributed throughout dolo-micrite matrix. In sample T23 detrital quartz was also found within vertical burrow wall. Overall abundant matrix has been divided into dolo-micrite (15% to 64%), micro- and pseudospar (10% to 19% - only in samples T24 and T22), plus clays and organics (trace in all samples). Pore filling cements were identified as calcite spar 1% to 5%), coarse crystalline dolomite (1% to 5%), plus pyrite (1% - only in sample T24). Trace to minor amounts of pyrite also acts as a replacement mineral of micrite, or microspar. All details in regards to mineralogical composition and proportions can be found in the Petrographic Summary Table 1.

Overall these four dolostone samples are tight. Samples T25, T23, and T22 show only trace amounts of intercrystalline, micro-intercrystalline, micro-vuggy, and fracture pores; however sample T24 does not show any visible porosity. The main porosity reducing features observed in these samples is the abundance of micrite that plugged primary interparticle pores, plus the recrystallization of some of the micrite to a tightly packed mosaic micro- and pseudospar. These samples also contain fair amount dolomite and calcite cement, which fills fractures, burrow walls, and replaces indistinct bioclast fragments.

Porosity as assessed by scanning electron microscope observation (SEM) is generally consistent with thin section observation. The pore system is characterized by scattered microporosity, often submicron pores, which occur in association with the micrite matrix. Porosity is absent where tightly interlocking crystal fabrics, which typically result from recrystallization, are dominant. Trace micro-intercrystalline (≤5µm) porosity noted in sample S23 is associated with probable bioclasts which have been replaced by rhombohedral dolomite cements.

Reservoir quality of the study dolostone samples is mainly controlled by diagenesis (i.e. mineral diagenesis and compaction) and to lesser extent by depositional environment (i.e. crystal and grain size of the precursor carbonate rock, burrowing of the sediment, etc.). Reservoir quality is was assessed as poor.

The following table summarizes the most important aspects that affected the reservoir quality of the four dolostone samples at the study location.

The following table summarize the most important factors that control the reservoir quality of the four samples recovered from B.A. TEXACO ARROWHEAD N-02 300/N-02-6040-12300/0 location.

| Sample ID | Depth (ft/m) | Total Micrite (%) | Total Cement & Replacement (%) | Total Porosity (%) | | | | | Main Porosity controlling factors (*) | RQ (*) |
|---|---|---|---|---|---|---|---|---|---|---|
| | | | | IP | Ixl | mV | Fr | M | | |
| **Location: B.A. Texaco Arrowhead N-02 300/N-02-6040-12300/00** | | | | | | | | | | |
| T25 | 13137.00/4004.16 | 64 | 3 | - | TR | - | TR | - | Mic; Com; Cc; Dc; Py; Br; C | P |
| T24 | 13147.50/4007.36 | 25 | 11 | - | - | - | - | - | Mic; Com; Ms; Cc; Dc; Py; C | P |
| T23 | 13162.10/4011.81 | 45 | 3 | - | - | TR | TR | TR | Mic; Com; Dc; Cc; Py; C; Br | P |
| T22 | 13681.80/4170.21 | 38 | 6 | - | TR | - | - | - | Mic; Com; Ms; Cc; Dc; Py | P |

**Porosity value (%):** **IP** – interparticle porosity; **Int** – intraparticle; **Ixl** – intercrystalline; **Mv** – micro-vuggy; **Fr** – fracture porosity; **M** – micro-intercrystalline porosity
**Main Porosity controlling factors:** **Com –** compaction (mechanical and chemical)**; Dol** – dolomitization; **Mic** – micrite (calcite or dolomite) and/or micritization; **Ms** – micro- and/or pseudospar; **Cc** – calcite cement (druse and spar); **Dc** – dolomite cement**; C** – clays and organics; **Qc** – quartz/chert cement; **Ov** – crinoid overgrowths; **Py** – pyrite (replacement and/or cement); **OM** – organic matter/pyrobitumen; **Dis** – dissolution; **F** – fabric: [**CC** – concavo-convex orthochem contacts; **S** – sutured orthochem contacts]; **Br** - burrowing
**RQ (*) - reservoir quality: VP –** very poor; **P –** poor; **M –** moderate; **G –** good

**Total Micrite: Note that the Total Micrite column includes micrite and also micro- and pseudospar replacement of micrite.**

Reservoir problems for the samples recovered from the Nahanni Formation at the B.A. Texaco Arrowhead N-02 300/N-02-6040-12300/0 location, may include the following: **(1)** isolated and small sizes of intercrystalline, micro-intercrystalline, micro-vuggy and fracture pores, plus overall poor interconnectivity between pores would restrict the flow and storage of hydrocarbons, **(2)** hydrochloric acid (HCl) treatment of this reservoir has the potential to loosen carbonate fines (dolo-micrite) that could migrate and block pore throats, plus cause fabric collapse, **(3)** the sensitivity of calcium carbonate to hydrofluoric acid (HF) in regard to precipitation of calcium fluoride scales.

In regards to overall poorly interconnected and heterogeneous pore system, fracture stimulation could be considered to create a more homogeneous production environment and to improve flow rates. After fracturing production rate should be held under a 'critical velocity' flow rate to avoid migration of formation fines created during fracturing.

Detailed mineralogical composition of each of the sample are summarized in the tables that can be find in the 'RESULTS' chapter of this report. Following the tabulated data there are images (with descriptions) that show specific features of the samples.

## METHODS

### Petrographic Microscopy

The thin section samples were cut from unclean core samples, and then impregnated with blue epoxy, polished and mounted onto a glass slide. After drying of the epoxy the samples were ground down to a total thin section thickness of 30μm. One half of each thin section was then stained with a combination of Alizarin Red (for calcite) and potassium ferricyanide (for ferroan carbonate) to highlight carbonate mineralogy, while the other half remained unstained. The dual carbonate stain helps to differentiate the carbonate components within the samples, and affects them as follows: calcite appear pink to red-brown, ferroan calcite shows mauve to blue, ferroan dolomite colors vary from pale blue to turquoise, while non-ferroan dolomite remains unstained. Finally a second glass slide was glued on the samples to protect the polished surface. The prepared thin sections were point counted (see the **Petrographic Summary Table 1**). The thin sections were examined in plain and cross polarized light conditions and photomicrographs taken at various magnifications (x12.5ppl; x25ppl; x50ppl, and x100ppl) to document structure, porosity, composition and nature of optically resolvable grains and matrix. To determine original texture of dolostone samples, the 'white card' technique has been used. Each sample has been described separately and the important features of it that includes framework mineralogy, diagenetic minerals and cements, textures, grain size range and average, porosity, etc., and the results are provided in the tabulated format. Annotated images of the thin sections with descriptions show the important aspects that were observed during the thin section examination. These images are placed after the tabulated data.

### SEM Analysis

A representative portion of each sample was adhered onto an aluminum stub specimen mount. The stubs were then sputter-coated with a conductive gold-palladium alloy for detailed Scanning Electron Microscopy (SEM) analysis and imaging. SEM analysis is useful in identifying lithological characteristics such as pore types, framework mineralogy, clay and cement composition, in addition to the potential deportment of clay constituents in relation to pore spaces and pore throats. Energy dispersive X-ray (EDX) was also used in conjunction with SEM observation in order to determine the elemental composition of the observed clay minerals and overall mineralogy.

<u>Bulk XRD Analysis</u>

Sample Preparation: Each sample, consisting of rock fragments, is manually crushed carefully using a mortar and pestle to reduce the size of the fragments. The sample is then ground with a vibratory disc mill (RS200; Retsch) to further reduce crystallite sizes. Finally, the sample is micronized using a planetary ball mill (PQN04; Across International) and scanned for X-ray diffraction analysis.

X-Ray Data Collection and Analysis:
Diffractometer Name: Bruker D4 Endeavor XRD with a Lynx-Eye detector
Instrumental Parameters: Radiation Source – Cobalt (Co)
Generator settings - 40 mA, 35 kV
Start position [°2θ] - 4
End position [°2θ] - 80
Step size [°2θ] - 0.02
Scan step time [s] - 1
Data Analysis: ICDD PDF-4 Mineral 2020 powder diffraction database
X'PERT HighScore Software for mineral identification
TOPAS Software for quantitative phase analysis
Detection Limit: 0.1 – 0.5 % depending on the type and nature of sample

Quantitative Mineral Phase Analysis: Using the HighScore program, the different mineral phases of the XRD patterns are identified. Once the mineral phases are identified, Rietveld refinements are performed by importing the XRD trace pattern into TOPAS 5. This program (TOPAS 5) is used for Rietveld analysis to quantify the mineralogy. The quantitative mineral phases of all samples are given in **Table 2**. The refined diffractograms and **Table 2** are placed in the **Tables and Figures** section of this report.

Texture and Grain Sizes

The scale for authigenic constituents in carbonates follows the Wentworth division, which is the most useful for dolomites, where transported particles are usually obliterated by replacement and crystal size is one of the few describable characteristic. The carbonate crystal sizes ranges are as follows: very fine crystalline (4 to 16μm), fine (16 to 62 μm), medium (62 to 250 μm), coarse (250-1000 μm), and very coarse crystalline (1000 to 4000 μm). The finest authigenic constituents are called cryptocrystalline (less than 1μm) and aphanocrystalline with the crystal size between 1 and 4 μm.

The following describes a division within the carbonate matrix. Micrite term is used for carbonate mud that consists of 1 to 4 μm diameter crystals and forms as an inorganic precipitate or through breakdown of coarser carbonate grains. Micrite is produced within the basin of deposition and shows little or no evidence of transport (Folk, 1959). Microspar is generally 5 to 20 μm sized calcite produced by recrystallization (neomorphism) of micrite and can be as coarse as 30 μm (Folk, 1965). Microspar is restricted to recrystallization products, not primary precipitates. Calcite fabric crystal size larger than 30 to 50 μm is called a pseudospar.

To describe detrital grains sizes, the Wentworth divisions will be used. The following is a list of actual size range for each Wentworth grain size: coarse silt (31 to 62.5μm), very fine (62.5 - 125μm), fine (125 - 250μm), medium (250 - 500μm), coarse (500- 1000μm), very coarse (1000 - 2000μm), plus granule (2000 - 4000μm) and pebble (>4000μm). The suffix 'lower' denotes that the grain size is toward the smaller portion of a specific size range, while the suffix 'upper' denotes that the grain size is toward the larger portion of a specific size range.

To describe the original texture of the rocks the modified Dunham (1962) classifications for carbonate rocks was used (see the figure below).

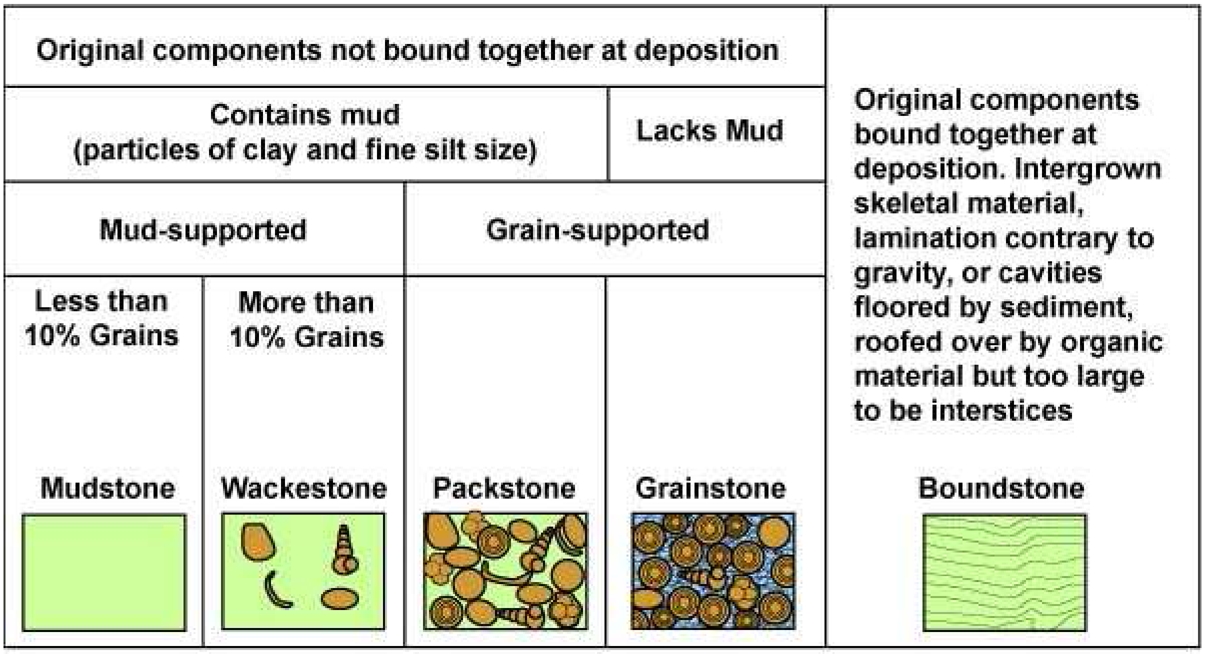


*C. G. St. C. Kendall, 2005 (after Dunham, 1962, AAPG Memoir 1)*

For the dolomite crystal fabrics the modified classification proposed by Sibley and Gregg (1987) was used (see the chart below).

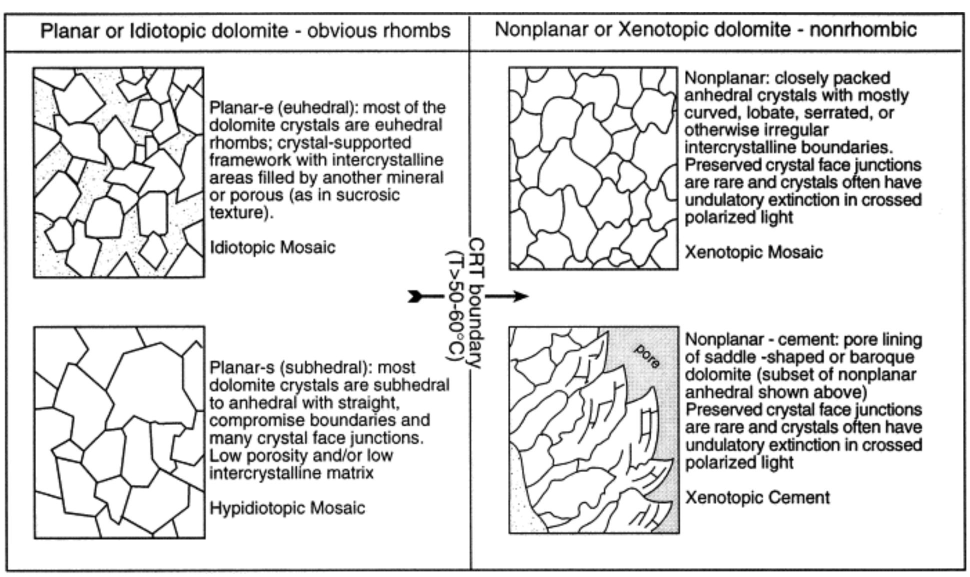

## Abbreviations

The list of common thin section abbreviations in provided in the table below.

| AME | ABBREVIATION | NAME | ABBREVIATION |
|---|---|---|---|
| Anhydrite | Anh | Intragranular Porosity | Intr. |
| Aphanocrystalline | Aph | Kaolinite | Kao |
| Barite | Ba | K-Feldspar | K-Fld |
| Biotite | Bio | Laminae | Lam |
| Bioclasts (indistinct) | Biocl | Metamorphic Rock Frag. | MRF |
| Burrows/Bioturbation | Bur | Muscovite | Musc |
| Bioturbation | Bt | Matrix | Mtx |
| Calcite | Cal | Micro-vuggy pore | mV |
| Carbonaceous | Carb | Organic material | OM |
| Chert | Cht | Phosphate | Phos |
| Chlorite | Chl | Plutonic Rock Fragments | PRF |
| Concavo-convex | CC | Polycrystalline quartz | PQ |
| Dolomite | Dol | Pseudo-matrix | P-mtx |
| Detrital Calcite | dC | Pyrite | Py |
| Detrital Dolomite | dD | Quartz | Qtz |
| Feldspar | Fld | Quartz Cement | Qc |
| Ferroan Dolomite | Fe-Dol | Quartz overgrowths | Ov |
| Ferroan Calcite | Fe-Cal | Sedimentary Rock Frag. | SRF |
| Glauconite | Glauc | Secondary porosity | SP |
| Grain dissolution pore | GD | Sutured grain contact | S |
| Heavy minerals | HM | Volcanic Rock Fragments | VRF |
| Hematite | Hem | | |
| Illite | Ill | | |
| Intergranular Porosity | IP | | |
| Intercrystalline Porosity | lxl | | |

## RESULTS

In this chapter of the report, the four samples that were recovered from the B.A. TEXACO ARROWHEAD N-02 300/N-02-6040-12300/0 location will be described separately. The images that show specific features of each sample will follow the tabulated sample description.

### Sample T25/S25/X43/P15, 10015.50ft/3052.72m

| | | | |
|---|---|---|---|
| **Well Name** | B.A. Texaco Arrowhead N-02 | **Location** | 300/N-02-6040-12300/0 |
| **Sample Type** | Thin section/SEM grain mount from a core sample | **Depth (ft/m)** | 10015.50ft/3052.72m |
| **Stratigraphic Unit** | Nahanni | **Reservoir Quality** | Poor |
| **Classification** | Dolostone (Mudstone) | **Stain type** | ½ Dual carbonate stain |

**MINERALOGY**

| Thin Section Point counting (%) | Total bulk mineralogy | | | | | |
|---|---|---|---|---|---|---|
| | Calcite | Dolomite | Quartz | Rock Fragments | Pyrite | Clays & organics |
| | 1 | 68 | 30 | TR | 1 | TR |
| | Framework, Matrix, Cement, and Replacement | | | | | |
| | Carbonate clasts | Bioclasts | Detrital grains | Matrix | Pore filling cement | Replacement |
| | 3 | - | 30 | 64 | 2 | 1 |

**ADDITIONAL FEATURES and OTHER COMMENTS**

| | |
|---|---|
| **Depositional** | The sample contains silty/sandy, slightly inclined laminae/lenses. Additionally indistinct burrows were also encountered. Fracturing occurred later in the diagenetic history of this mudstone and the majority of the fractures have been healed with coarse crystalline dolomite and calcite. |
| **Textures** | Based on the mineralogy and proportion between framework components (carbonate clasts and bioclasts) and matrix, the sample was classified as limestone-mudstone. For the matrix, the crystal texture has been determined as anhedral, while cement shows subhedral to euhedral crystal texture. |
| **Framework (Carbonate clasts, Bioclasts)** | Petrographic Summary Table 1 shows that allochems are represented solely by carbonate clasts and include intraclasts (2%), peloids (1%), plus trace ooids. There are no bioclasts in this sample. |
| **Detrital Grains & Other Non-Carbonate Grains** | Detrital grains occur mainly as quartz silt to sand sized grains (30%). Additionally trace amounts of plutonic rock fragments were also detected (see Figure 2). |
| **Matrix** | Abundant matrix comprises dolo-micrite (64%), plus trace amounts of clays and organic material. |
| **Pore Filling Cements** | The pore filling cements occur in minor amounts and include calcite spar (1%) and dolomite (1%). |

| | |
|---|---|
| **Replacement Minerals** | Minor amounts of pyrite (1%) is locally intermixed with organic material. Additionally pyrite also replaces micrite within the matrix and micritized framework grains. |
| **Porosity** | There is only a trace visible porosity that include intercrystalline and fracture porosity. Helium porosity of the core plug was measured as 0.5%., while gas permeability is 0.65md. |

Three thin section and four SEM annotated microphotographs with descriptions are provided below.

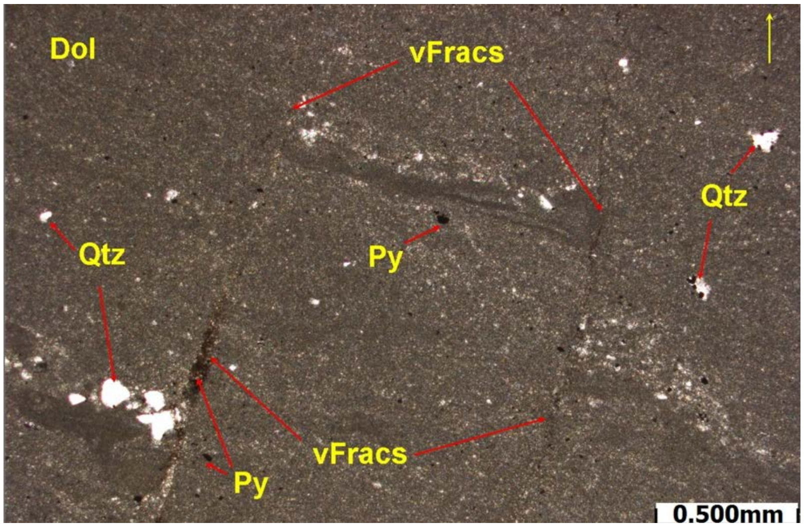


**Figure 1.1. Sample T25, 10015.50ft/3052.72m**. This image focuses on the presence of micro-vertical fractures (vFracs) that are actually a micro-faults (note a displacement of dark brown micritic and sandy laminae). Pyrite (Py) framboids partly replace dolo-micrite (Dol), plus have also healed the vertical fracture. The quartz silt and sand sized grains are usually incorporated into discontinued laminae and lenses. **x50ppl**

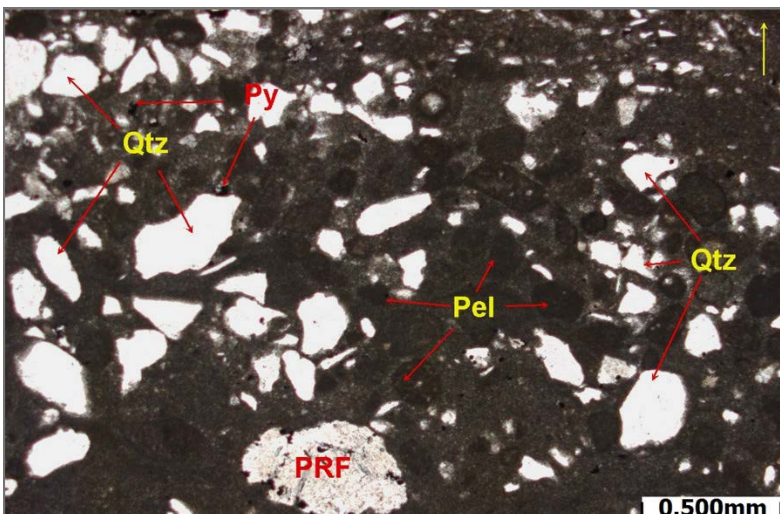


**Figure 1.2. Sample T25, 10015.50ft/3052.72m**. Another moderate magnification image shows the interior of laminae/lens that contain mainly monocrystalline quartz (Qtz) and peloids (Pel), plus rare plutonic rock fragments (PRF). The groundmass is composed of dolo-micrite. Note a big variation in detrital grain sizes (silt to medium grained). Peloids are much smaller and more uniform in regards to the sizes than detrital grains. Pyrite framboids (Py) locally replace micrite matrix. There is no visible porosity in this image. **x50ppl**

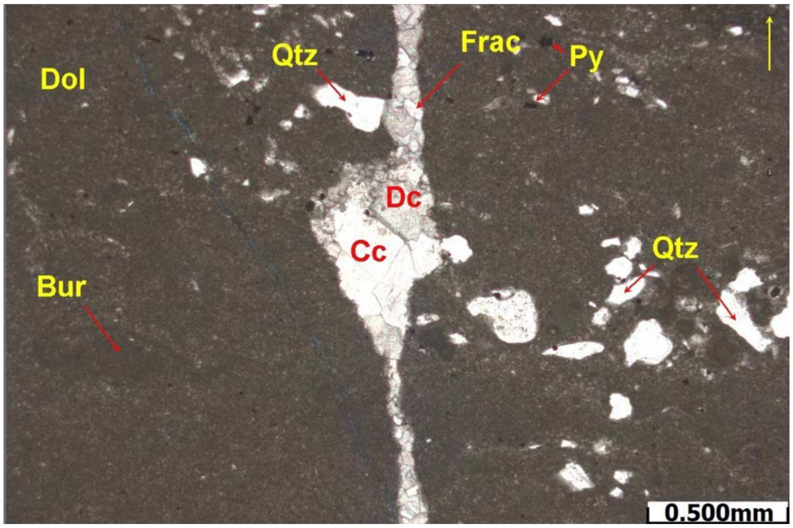


**Figure 1.3. Sample T25, 10015.50ft/3052.72m**. Tis image highlight a vertical fracture (Frac). That has been totally filled vith dolomite (Dc) followed by calcite spar cement (Cc). Detrital quartz (Qtz) grains appear to be randomly distibuted throughout dolo-micrite matrix (Dol). Indistinct horizontal burrows have slightly darker color (organic-rich micrite?) than the surrounding matrix. Scattered pyrite framboids (Py) replace dolo-micrite. **x50ppl**

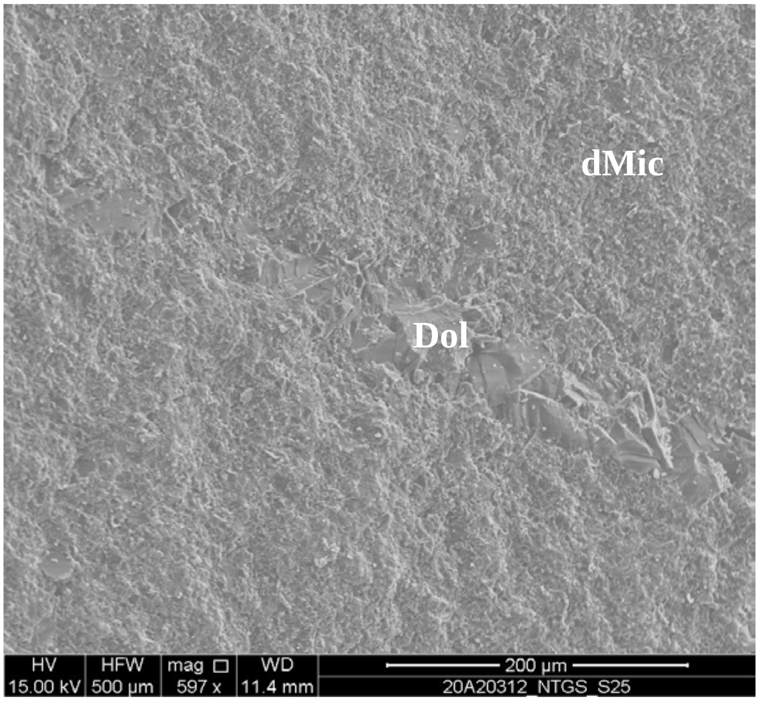


**SEM Figure 1.5. Sample S25, 10015.50ft/3052.72m**. Low magnification overview of vein- or fracture-fill which consists of fine crystalline dolomite (Dol). dMic: dolomicrite/aphanocrystalline dolomite. **x597**

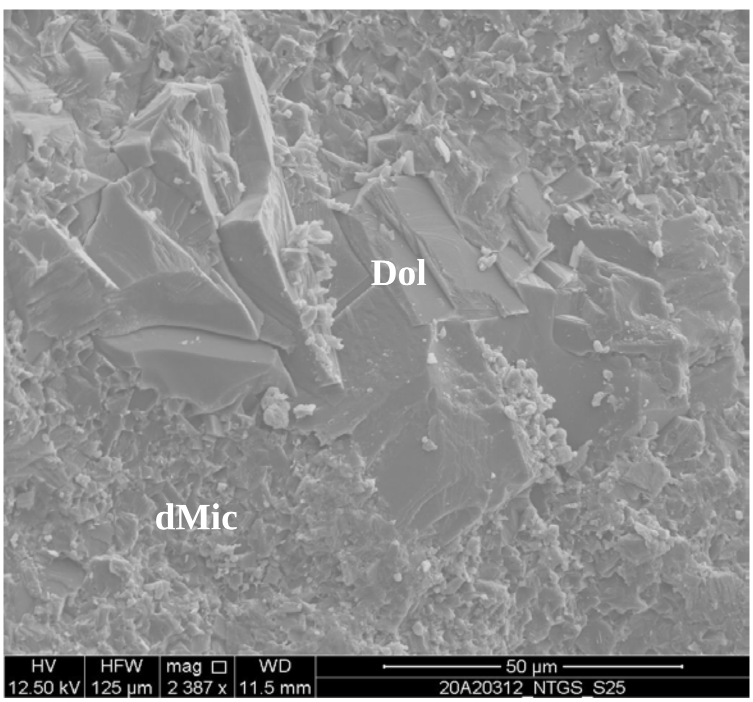


**SEM Figure 1.6. Sample S25, 10015.50ft/3052.72m**. Higher magnification image showing details of dolomite (Dol) vein-fill as shown in **Figure 1.5**. Porosity is poorly preserved due to the tightly interlocking crystal fabric of the fine sub- to euhedral dolomite rhombs. However, visible microporosity is present within the dolomicrite/aphanocrystalline matrix (dMic) at high magnifications (**see Figure 1.8**). **x2387**

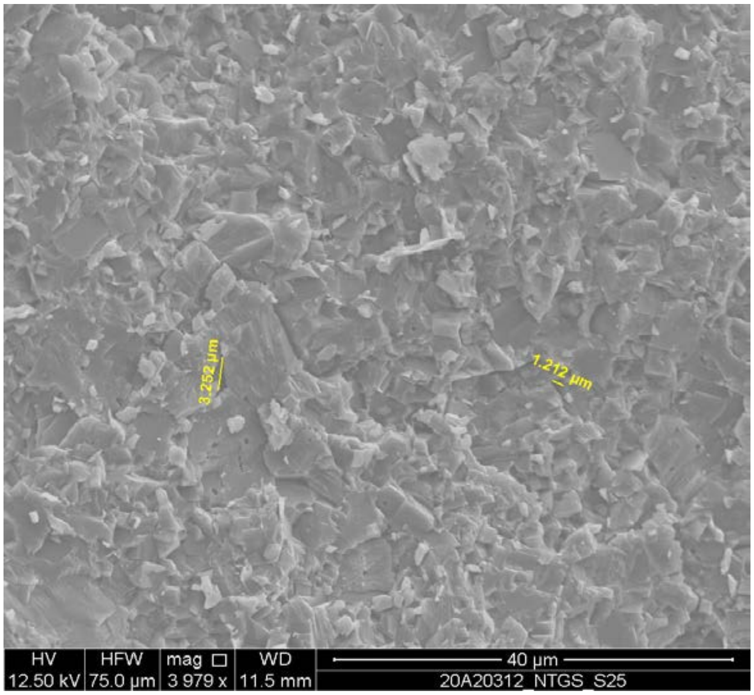


**SEM Figure 1.7. Sample S25, 10015.50ft/3052.72m**. This moderate magnification image features microporosity (<5µm) within the very fine to aphanocrystalline dolomite matrix. **x3979**

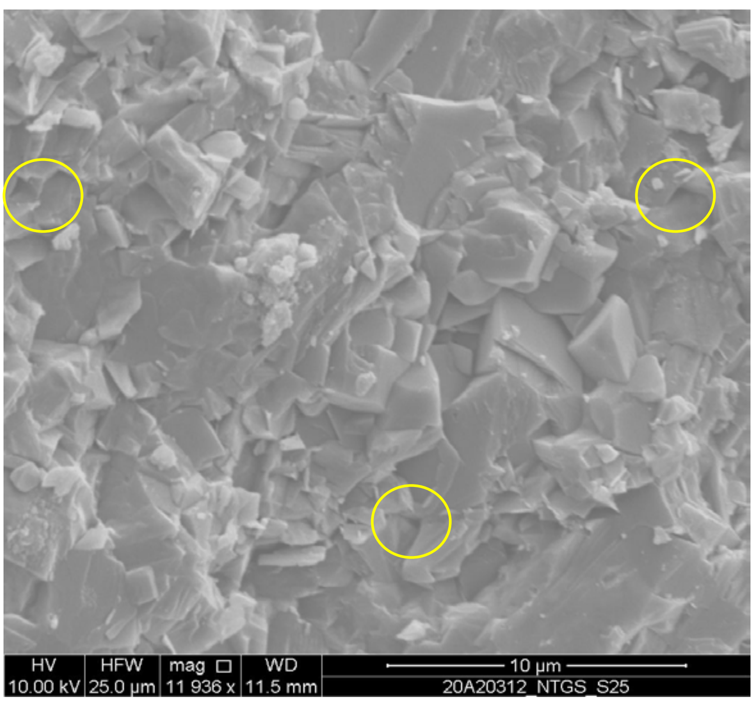


**SEM Figure 1.8. Sample S25, 10015.50ft/3052.72m**. High magnification image of the aphanocrystalline (<4µm) matrix. Scattered submicron pores are highlighted with yellow circles within this view. **x11936**

## Sample T24/S24/X42/P14, 10020.00ft/3054.10m

| | | | |
|---|---|---|---|
| **Well Name** | B.A. Texaco Arrowhead N-02 | **Location** | 300/N-02-6040-12300/0 |
| **Sample Type** | Thin section/SEM grain mount from a core sample | **Depth (ft/m)** | 10020.00ft/3054.10m |
| **Stratigraphic Unit** | Nahanni | **Reservoir Quality** | Poor |
| **Classification** | Dolostone (Packstone-Wackestone) | **Stain type** | ½ Dual carbonate stain |

**MINERALOGY**

| Thin Section Point counting (%) | Total bulk mineralogy | | | | | |
|---|---|---|---|---|---|---|
| | Calcite | Dolomite | Quartz | Pyrite | Clays & organics | |
| | 5 | 94 | - | 1 | TR | - |
| | Framework, Matrix, Cement, and Replacement | | | | | |
| | Carbonate clasts | Bioclasts | Detrital grains | Matrix | Pore filling cement | Replacement |
| | 20 | 44 | - | 25 | 11 | TR |

**ADDITIONAL FEATURES and OTHER COMMENTS**

| | |
|---|---|
| **Depositional** | At the time of deposition, the sample was most likely massive. Occasional microfractures most likely formed during burial diagenesis. |
| **Textures** | Based on the mineralogy and proportion between framework components (carbonate clasts and bioclasts) and matrix, the sample was classified as lime mudstone to wackestone. For the matrix, the crystal texture has been determined as anhedral, while cement shows subhedral to euhedral crystal texture. Majority of bioclasts are highly fragmented and micritized and/or cemented with dolomite and calcite spar or microspar. |
| **Framework (Carbonate clasts, Bioclasts)** | Petrographic Summary Table 1 shows detailed mineralogy of the sample. This sample contains 94% of dolomite, plus minor amounts of calcite (5%) and pyrite (1%). Trace amounts of clays/organic material is also present in this sample. Dolomite occurs mainly as bioclasts [annelid worms - 25%, brachiopod – 10%, indistinct - 5%, mollusks – 4%, plus trace ostracodes] and as carbonate clasts [peloids – 20%,]. Note that abundant amounts of dolomite is also present within the matrix. |
| **Detrital Grains & Other Non-Carbonate Grains** | There are no detrital grains in this sample. |
| **Matrix** | Dolomite is the main component of the matrix (25%), while clays and organics occur in trace amounts. It should be noted that the dolomite matrix is divided into dolo-micrite (15%) and microspar (10%). Microspar and/or pseudospar has formed after recrystallization of micrite. |
| **Pore Filling Cements** | The pore filling cements occur in moderate amounts and include calcite and dolomite spar (5% of each), plus pyrite (1%). |
| **Replacement Minerals** | Trace amounts of pyrite also acts as a replacing agent of micrite. |
| **Porosity** | There is no visible porosity in this sample. Note that the helium porosity measured on core plug is reported by RCA as 1.4% with the permeability of 0.12mD. |

Annotated microphotographs of the thin section and SEM samples with descriptions are provided below.

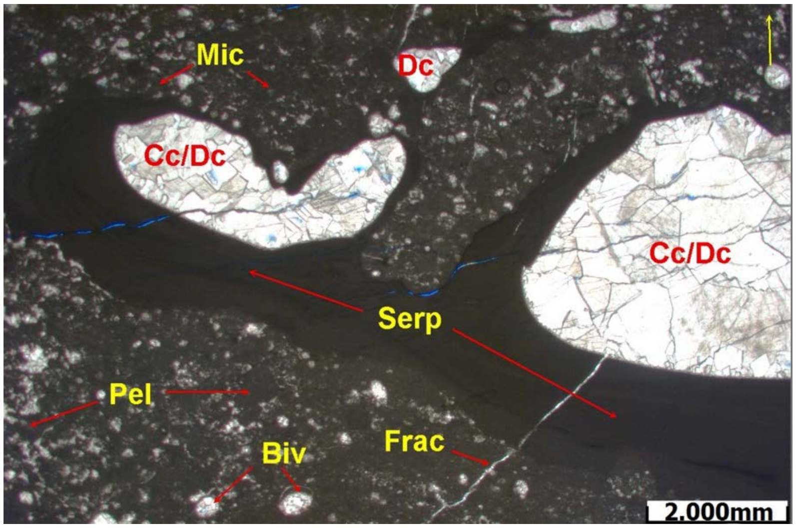


**Figure 2.1. Sample T24, 10020.00ft/3054.10m.** Low magnification overview of the sample highlights the presence of a annelid worm (possible serpulid). Serpulid (Serp) worm tubes appear encrusting on mollusks shells and upon each other. The soft body of mollusks have been dissolved and subsequently cemented by euhedral dolomite, followed by later calcite spar (Cc/Dc). The tubes are dense and have laminar wall structure. The serpulid tubes are surrounded by peloidal-skeletal dolo-packstone to dolo-wackestone matrix (Pel; Biv). Frac: micro-fracture. **x12.5ppl**

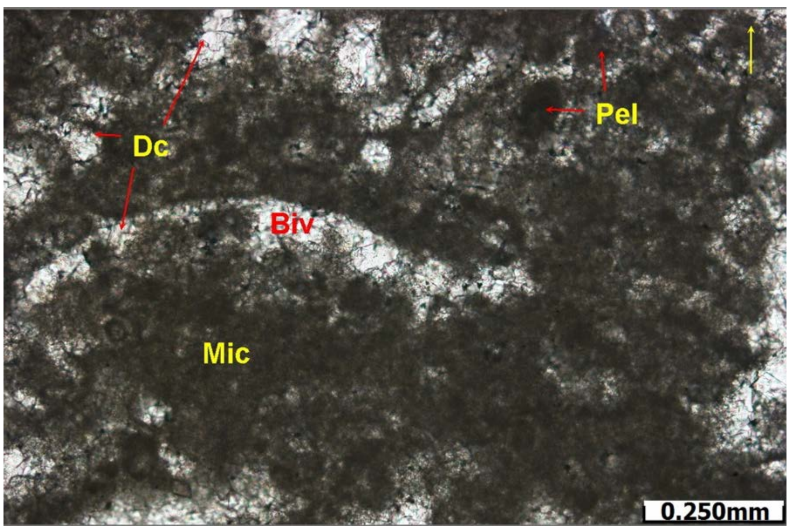


**Figure 2.2. Sample T24, 10020.00ft/3054.10m.** High magnification image of the sample shows carbonate grains (peloids – Pel) and indistinct bivalve (Biv) shell fragments floating in dolo-micrite matrix (Mic). Peloids are composed of dolo-micrite as well. The bioclast shell fragments have been replaced with blocky dolomite cement (Dc). **x100ppl**

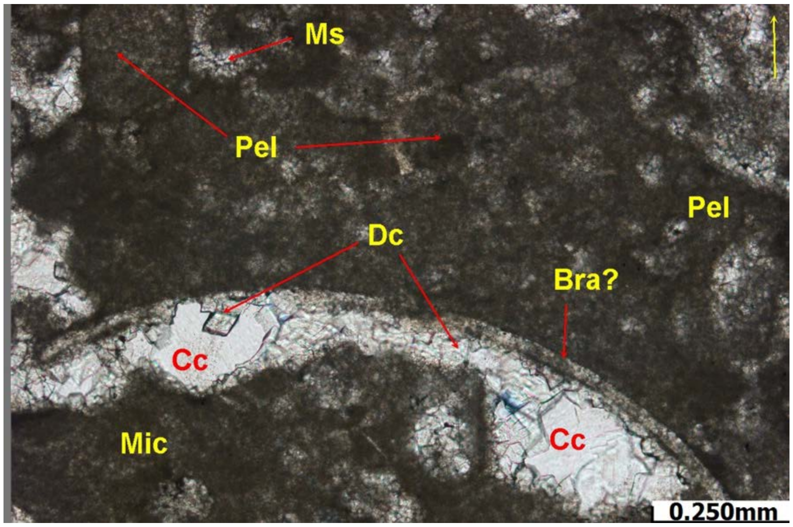


**Figure 2.3. Sample T24, 10020.00ft/3054.10m.** Another high magnification image of the sample shows an abundance of peloids (Pel) with occasional possible brachiopod shell fragments (Bra?). The shell is replaces by dolomite rhombs (Dc) followed by the diagenetically later calcite spar (Cc). The micritic matrix has recrystallized into mosaic of micro- and pseudospar (MS) that totally plugs the primary interparticle pores. **x100ppl**

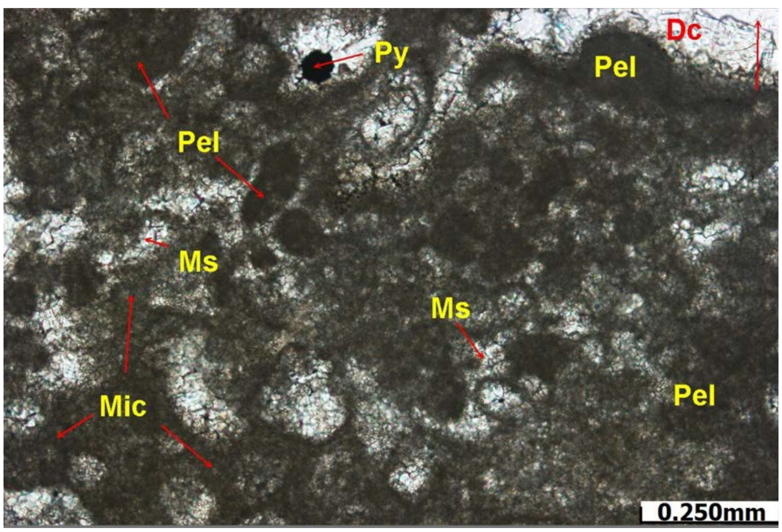


**Figure 2.4. Sample T24, 10020.00ft/3054.10m.** High magnification image shows the peloidal-skeletal groundmass of this sample. The majority of the carbonate grains are peloids (Pel) the primary dolo-micrite matrix (Mic) has been greatly recrystallized to tight microspar (Ms) and pseudospar. Occasionally late pyrite (Py) forms inclusions (replaces) microspar. Dolomite cement (Dc) has most likely replaced indistinct bioclast fragment. x1**00ppl**

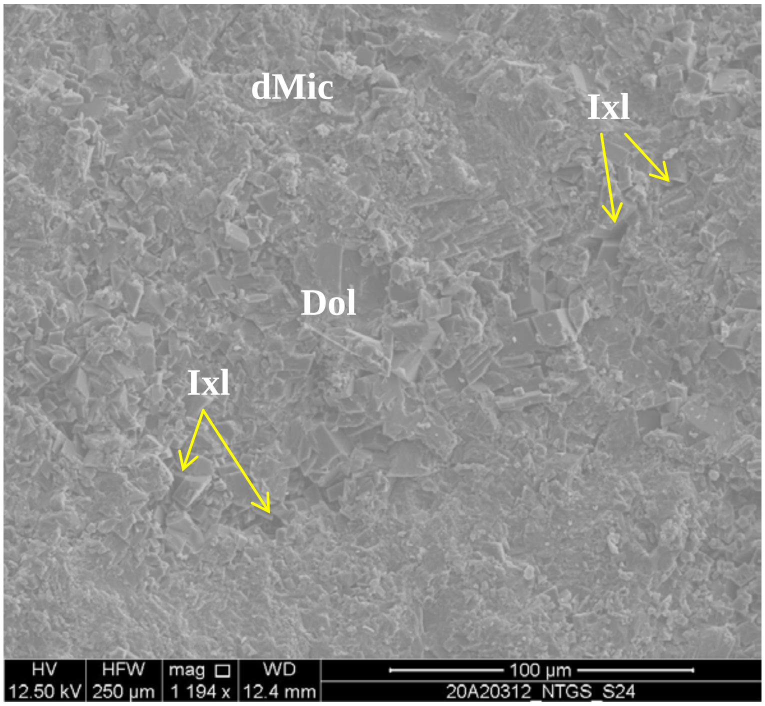


**SEM Figure 2.5. Sample S24, 10020.00ft/3054.10m.** High magnification overview highlighting patchy fine crystalline dolomite (Dol) within the dolomicrite/aphanocrystalline matrix (dMic). Localized well-connected intercrystalline porosity (Ixl) is associated with fine crystalline dolomite, while visible pore spaces within this view range in size from <1µm to 6µm. **x1194**

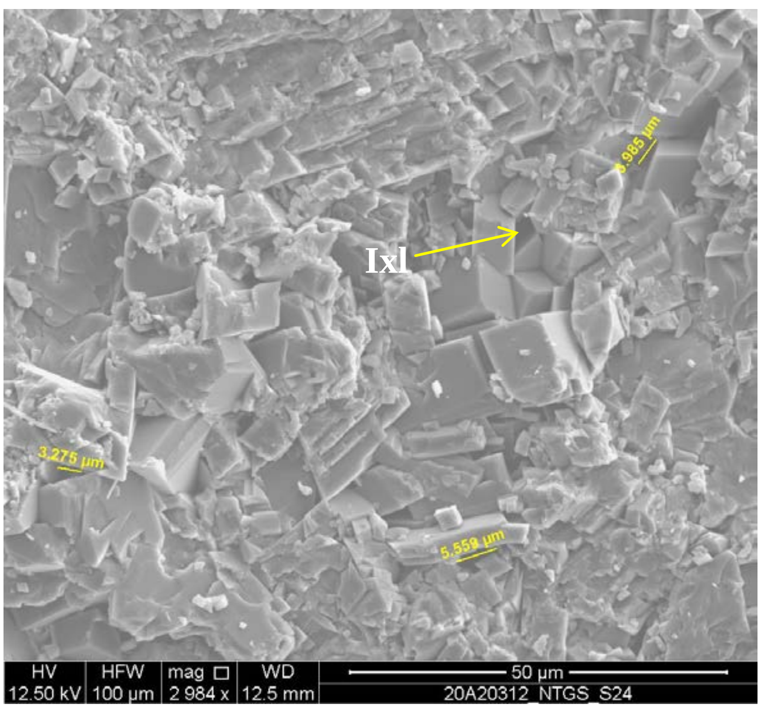


**SEM Figure 2.6. Sample S24, 10020.00ft/3054.10m.** Moderate magnification view showing details of patchy fine crystalline dolomite as shown in the overview image (**Figure 2.5**). Locally well-connected intercrystalline porosity (Ixl) ranges in size from <1µm to 6µm, and appears to be ~3µm. **x2984**

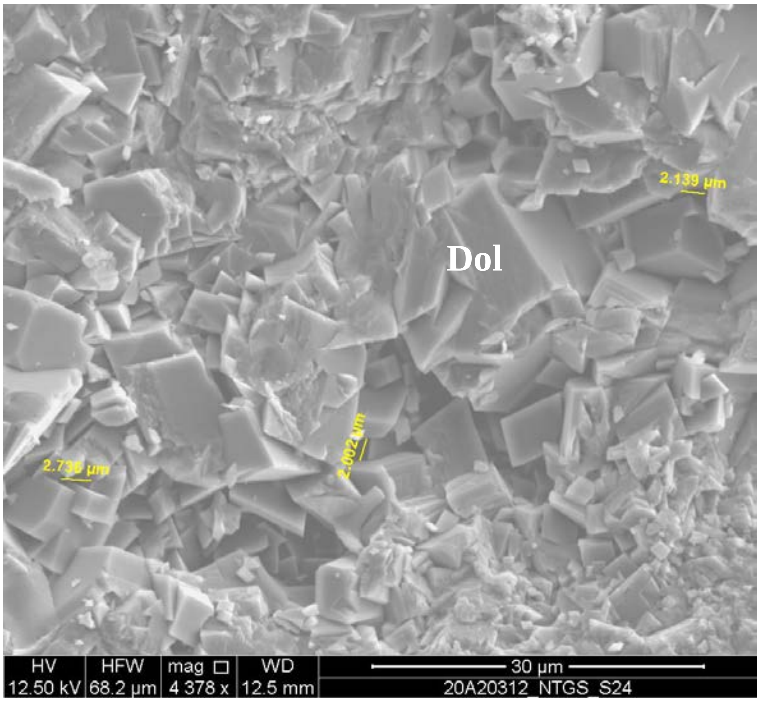


**SEM Figure 2.7. Sample S24, 10020.00ft/3054.10m.** Moderate magnification view showing the variable crystal sizes of the sub- to euhedral dolomite rhombs (Dol). The lower right-hand portion of the image shows the aphanocrystalline matrix which dominates the sample, while dolomite within the upper right-hand portion of the image ranges in size from very fine to fine crystalline. The average intercrystalline pore size within this view is ~2µm. **x4378**

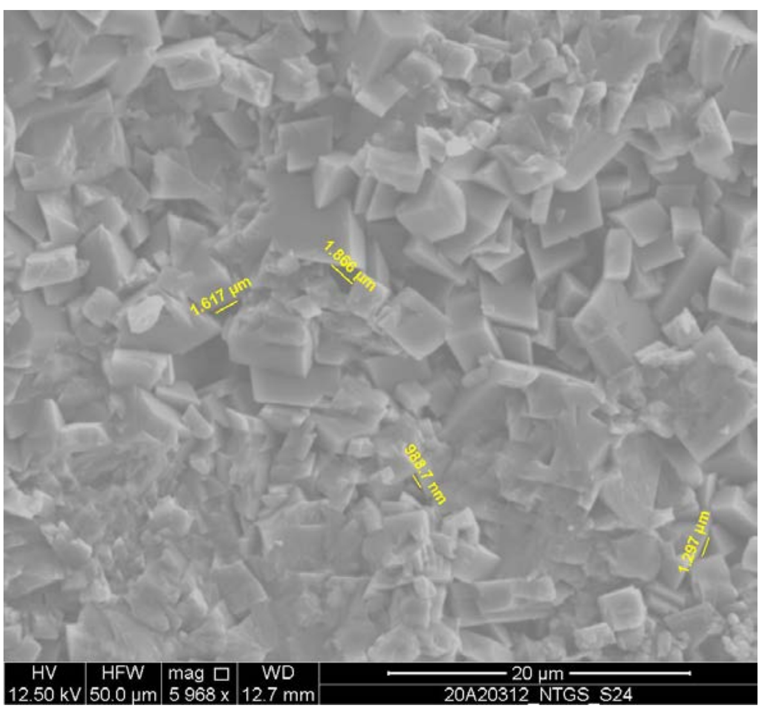


**SEM Figure 2.9. Sample S24, 10020.00ft/3054.10m.** High magnification view of localized well-connected microporosity (<5µm). **x5968**

## Sample T23/S23/X41/P13, 10023.75ft/3055.24m

| | | | |
|---|---|---|---|
| **Well Name** | B.A. Texaco Arrowhead N-02 | **Location** | 300/N-02-6040-12300/0 |
| **Sample Type** | Thin section/SEM grain mount from a core sample | **Depth (m)** | 10023.75ft/3055.24m |
| **Stratigraphic Unit** | Nahanni | **Reservoir Quality** | Poor |
| **Classification** | Dolostone (Mudstone-Wackestone-Packstone) | **Stain type** | ½ Dual carbonate stain |

**MINERALOGY**

| Thin Section Point counting (%) | Total bulk mineralogy | | | | | |
|---|---|---|---|---|---|---|
| | Calcite | Dolomite | Quartz | Pyrite | Clays & organics | |
| | 1 | 84 | 15 | TR | TR | - |
| | Framework, Matrix, Cement, and Replacement | | | | | |
| | Carbonate clasts | Bioclasts | Detrital grains | Matrix | Pore filling cement | Replacement |
| | 35 | 2 | 15 | 45 | 3 | TR |

**ADDITIONAL FEATURES and OTHER COMMENTS**

| | |
|---|---|
| **Depositional** | At the time of deposition, the sample was most likely massive and moderately to heavily burrowed/bioturbated (indistinct horizontal and vertical burrows). Development of low amplitude stylolites and fracturing of the sediment typically happens during burial diagenesis (mechanical and chemical compaction). |
| **Textures** | Mineralogically the sample a dolostone (84% of dolomite) that has mudstone to wackestone and to packstone texture. For the matrix, the crystal texture has been determined as anhedral, while cement shows subhedral to euhedral crystal texture. |
| **Framework (Carbonate clasts, Bioclasts)** | Dolomite is a dominant mineral (84% of the total rock volume). Moderate amounts of detrital quartz (15%), minor calcite (1%), plus trace pyrite and clays/organic matter are the other minerals (see Petrographic Summary Table 1). The framework builders are represented mainly by carbonate clasts [peloids – 35%, plus trace ooids and intraclasts], with minor bioclasts [corals – 1%, indistinct bioclasts – 1%, plus trace ostracodes]. |
| **Detrital Grains & Other Non-Carbonate Grains** | Detrital grains occur as monocrystalline quartz silt and sand sized grains. |
| **Matrix** | Dolo-micrite (45%) is the matrix of this sample with trace amounts of clays and organic material. |
| **Pore Filling Cements** | The pore filling cements occur in minor amounts and include calcite (1%) and dolomite (2%) spar. |
| **Replacement Minerals** | Trace amounts of pyrite is the replacing agent of micrite and micritized framework. |
| **Porosity** | There is only a trace amount of micro-vuggy, fracture and micro-intercrystalline porosity in this sample. The RCA helium porosity that was measured on core plug is reported as 0.7%. The gas permeability of the core sample is 0.06mD. |

The next pages show annotated microphotographs of the thin section and SEM sample with descriptions.

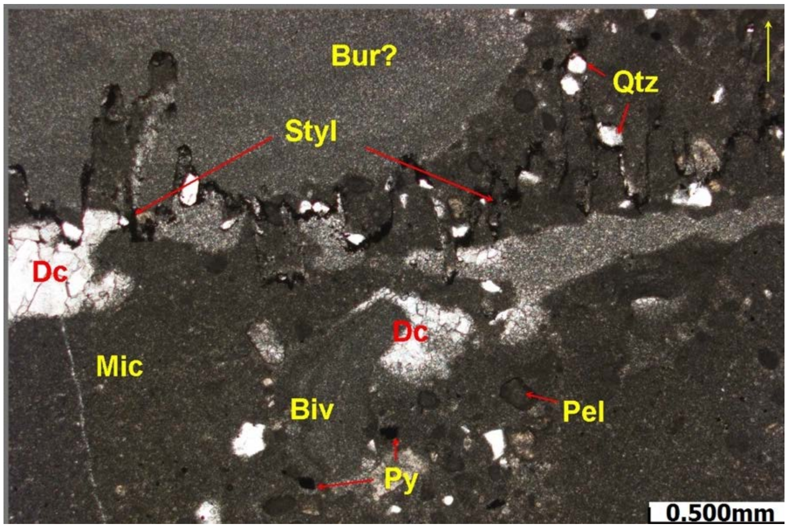


**Figure 3.1. Sample T23, 10023.75ft/3055.24m.** Moderate magnification image of the thin section focuses on low to moderate amplitude micro-stylolite that cuts through this sample. The framework builders in this image include peloids (Pel) and micritic bivalve fragments (Biv). Detrital quartz silt is scattered throughout dolo-micrite (Mic) groundmass. Note that burrows (Bur?) are also filled with micrite. Possible micro-vuggy pores created by dissolution of framework components have been filled with dolomite spar cement (Dc). Pyrite (Py) framboids replace micrite. **x50ppl**

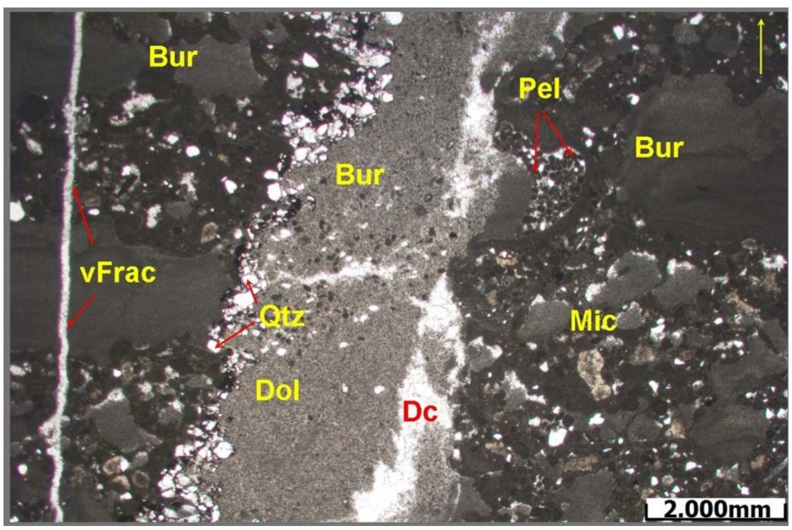


**Figure 3.2. Sample T23, 10023.75ft/3055.24m**. Low magnification image of the burrowed (Bur) dolostone sample shows large sized vertical burrow (middle), plus a few horizontal burrows, Note the difference in color of the backfill, which is dolo-micrite – Dol) of the vertical (light) and the other burrows (dark). The matrix in this image consists of micrite (Mic) with scattered peloids (Pel) and detrital quartz (Qtz) grains. The walls of the vertical burrow are filled with marked with quartz silt (left) and blocky to spar dolomite (Dc). Vertical micro-fracture (vFrac) is healed with dolomite druse. Note that loosely packed burrows can act as significant conduits for diagenetic fluid flow. **x12.5ppl**

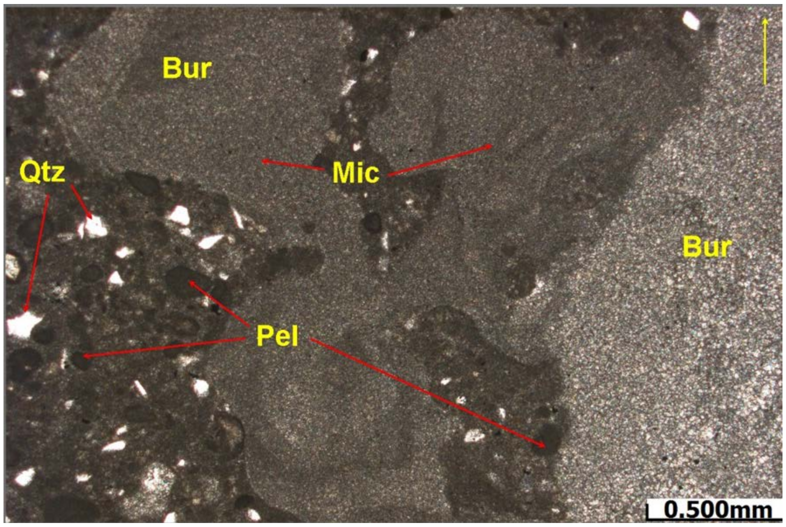


**Figure 3.3. Sample T23, 10023.75ft/3055.24m.** Moderate magnification image shows irregularly shaped burrows (Bur) surrounded by peloidal wackestone-mudstone matrix. Both burrows fill and the matrix are composed of micrite (Mic). Quartz silt and sand sized detrital grains (Qtz) are scattered throughout the matrix. There is no visible porosity in this image. **x50ppl**

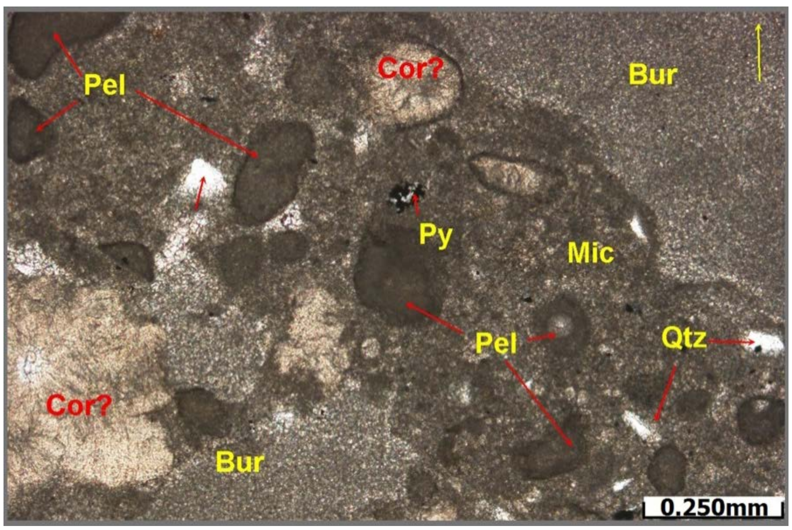


**Figure 3.4. Sample T23, 10023.75ft/3055.24m.** High magnification image of the sample shows the framework components with peloids (Pel) and occasional calcitic coral fragments (Cor?). The groundmass is composed of dolo-micrite (Mic), which is locally replaced by pyrite framboids (Py). White grains observed in this image were identified as detrital quartz (Qtz). The backfill of the burrows is much lighter (possibly more porous) than the micrite matrix. **x100ppl**

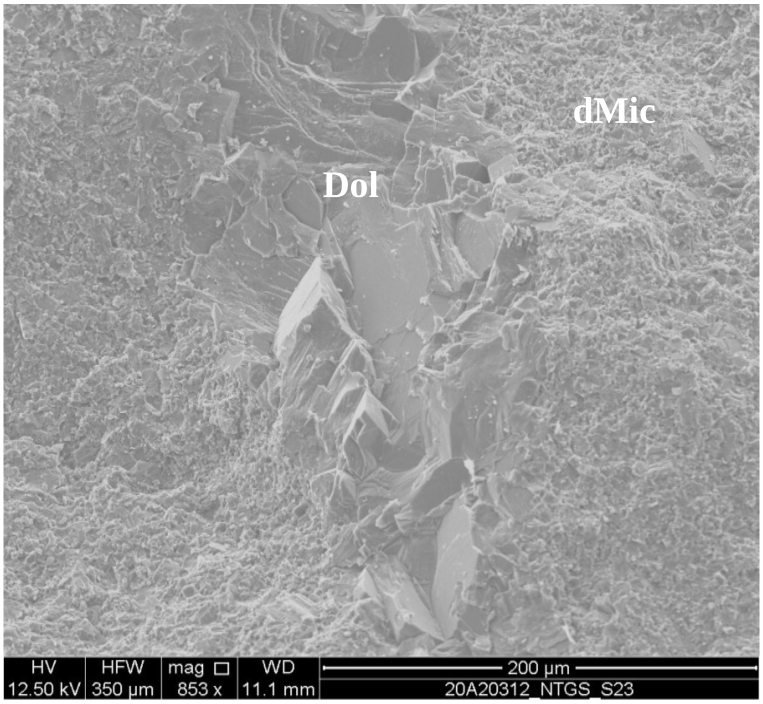


**SEM Figure 3.5. Sample S23, 10023.75ft/3055.24m.** Low magnification overview image highlighting medium crystalline replacement dolomite (Dol) within an aphanocrystalline/dolomicritic matrix (dMic). Visual porosity is poor within this sample. Scattered submicron pores were identified in association with the matrix (**see Figure 3.7**). **x853**

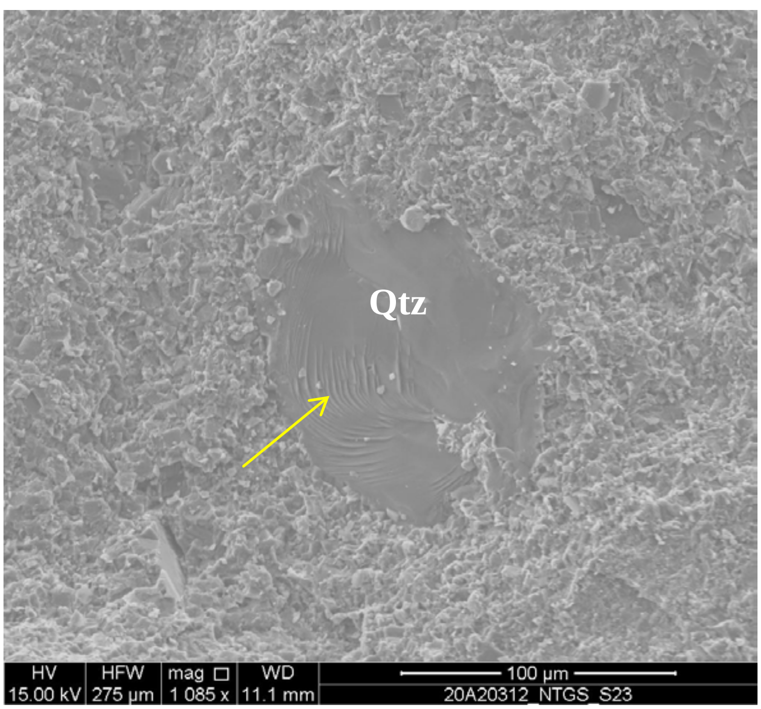


**SEM Figure 3.6. Sample S23, 10023.75ft/3055.24m.** Moderate magnification view of a very fine detrital quartz grain displaying conchoidal fracture patterns (yellow arrow). **x1805**

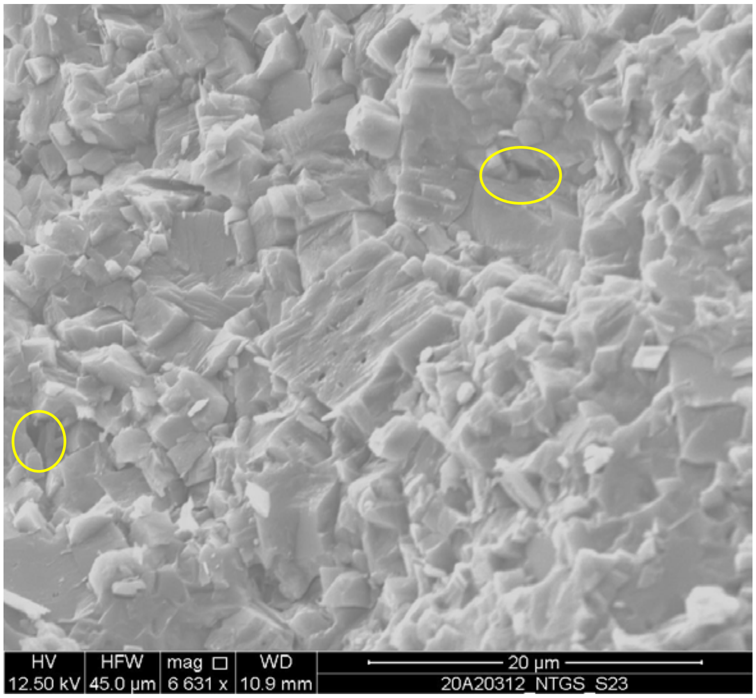


**SEM Figure 3.7. Sample S23, 10023.75ft/3055.24m.** High magnification view of aphanocrystalline to very fine crystalline dolomite that comprises the matrix. Scattered submicron intercrystalline pore spaces are highlighted with yellow circles within this view. **x6631**

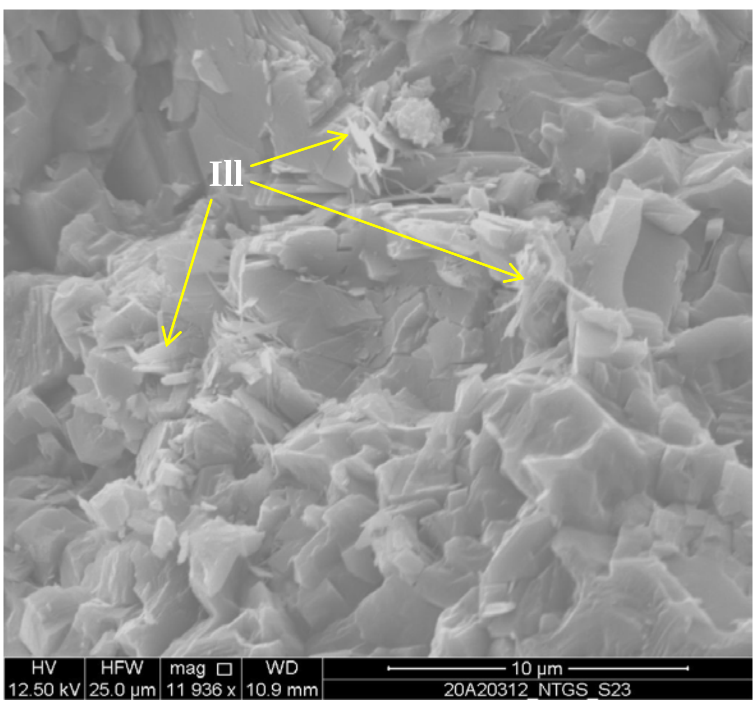


**SEM Figure 3.8. Sample S23, 10023.75ft/3055.24m.** High magnification view of wispy filamentous illite (Ill). Clays were only noted in trace amounts within this sample. **x11936**

## Sample T22/S22/X40/P12, 10042.20ft/3060.86m

| | | | |
|---|---|---|---|
| **Well Name** | B.A. Texaco Arrowhead N-02 | **Location** | 300/N-02-6040-12300/0 |
| **Sample Type** | Thin section/SEM grain mount from a core sample | **Depth (m)** | 10024.20ft/3060.86m |
| **Stratigraphic Unit** | Nahanni | **Reservoir Quality** | Poor |
| **Classification** | Dolostone (Wackestone-Packstone) | **Stain type** | ½ Dual carbonate stain |

**MINERALOGY**

| Thin Section Point counting (%) | Total bulk mineralogy | | | | | |
|---|---|---|---|---|---|---|
| | Calcite | Dolomite | Quartz | Pyrite | Clays & organics | |
| | 4 | 96 | - | TR | TR | - |
| | Framework, Matrix, Cement, and Replacement | | | | | |
| | Carbonate clasts | Bioclasts | Detrital grains | Matrix | Pore filling cement | Replacement |
| | 31 | 25 | - | 38 | 6 | TR |

**ADDITIONAL FEATURES and OTHER COMMENTS**

| | |
|---|---|
| **Depositional** | The sample is throughout laminated. Dark laminae contain mainly dolo-micrite with scattered carbonate clasts and bioclasts, while the lighter laminae consists predominantly microspar. Geopetal structures are locally observed with partly leached ostracod shell fragments (see Figure 4.1). Fracturing of the sediment (overall very minor) happened during burial diagenesis. |
| **Textures** | Mineralogically the sample a dolostone (84% of dolomite) that has mudstone to wackestone and to packstone texture. For the matrix, the crystal texture has been determined as anhedral, while cement shows subhedral to euhedral crystal texture. |
| **Framework (Carbonate clasts, Bioclasts)** | Dolomite is a dominant mineral (84% of the total rock volume). Moderate amounts of detrital quartz (15%), minor calcite (1%), plus trace pyrite and clays/organic matter are the other minerals (see Petrographic Summary Table 1). The framework builders are represented mainly by carbonate clasts [peloids – 35%, plus trace ooids and intraclasts], with minor bioclasts [corals – 1%, indistinct bioclasts – 1$%, plus trace ostracodes]. |
| **Detrital Grains & Other Non-Carbonate Grains** | There are no detrital grains in this sample. |
| **Matrix** | The matrix of this sample has been divide into three components: dolo-micrite (19%), microspar (19%), and clays and organics (trace). |
| **Pore Filling Cements** | The pore filling cements include equal amounts of calcite spar, calcite druse and dolomite (2% of each). |
| **Replacement Minerals** | Trace amounts of pyrite is the replacing agent of micrite and micritized framework. |
| **Porosity** | There is only a trace amount of intercrystalline porosity in this sample. The RCA helium porosity that was measured on core plug is reported as 0.9%. The gas permeability of the core sample is 0.01mD. |

The next pages show annotated microphotographs of the thin section and SEM sample with descriptions.

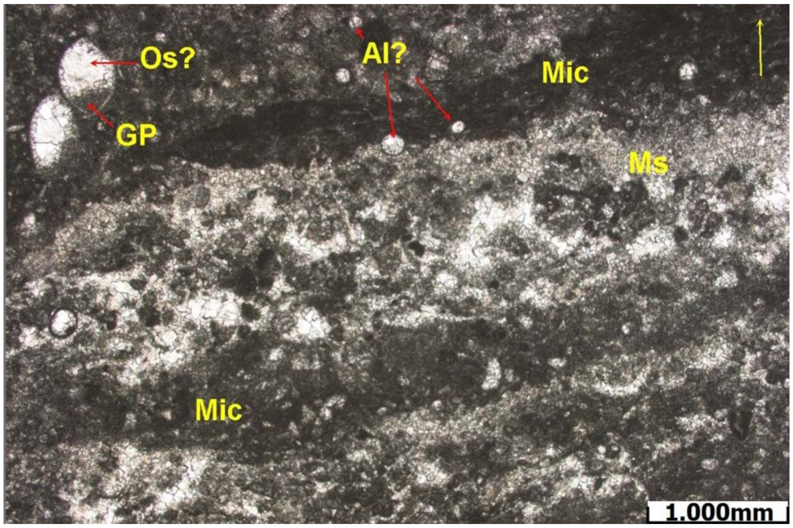


**Figure 4.1. Sample T22, 10042.20ft/3060.86m.** Moderate magnification image of laminated dolo-wackestone to packstone. The light color laminae are mainly micrite that has been recrystallized to tight packed mosaic microspar (Ms). The dark laminae comprise dolo-micrite with scattered carbonate clasts (peloids and intraclasts) and bioclasts such as mollusks fragments, algae (Al?), ostracodes (Os?) and indistinct highly fragmented and micritized bioclasts fragments. Note geopetal structure (GP) within partly cemented ostracode shell fragments **x25ppl**

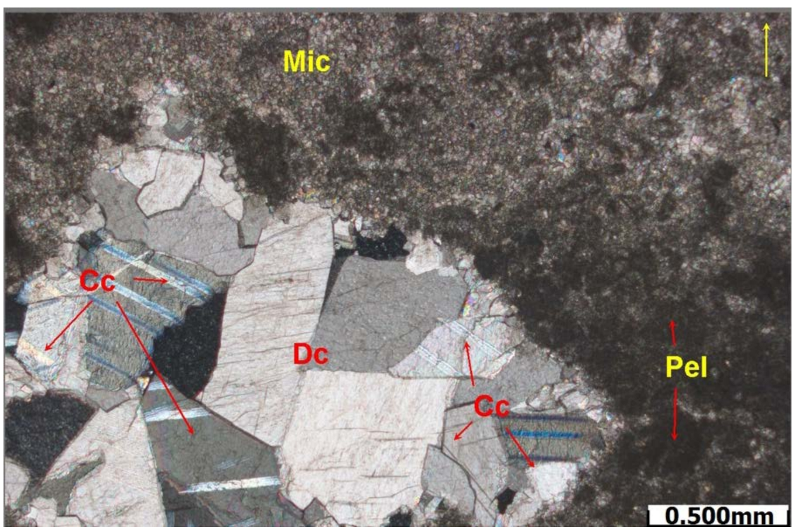


**Figure 4.2. Sample T22, 10042.20ft/3060.86m.** Another moderate magnification image of the sample was taken under cross polarized light condition to show two generations of cements that fill dissolution enlarged intrafossil or micro-vuggy pore. The void has been filled with dolomite spar (Dc) and then by calcite spar (Cc) that has partly replaced dolomite cementation. Dolomicrite (Mic) with scattered peloids (Pel) is the matrix of this sample. **x50xpl**

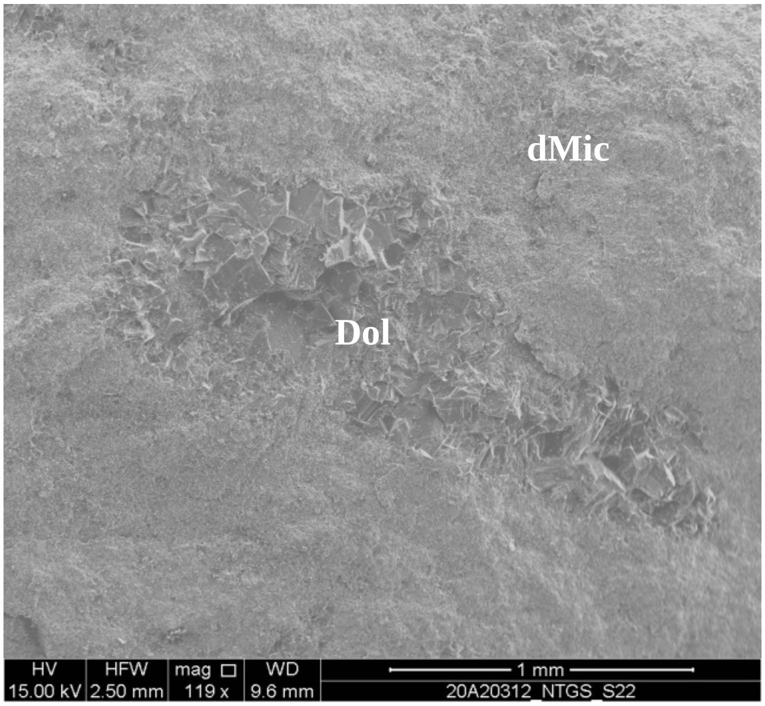


**SEM Figure 4.3. Sample S22, 10042.20ft/3060.86m.** Low magnification overview of the dolostone showing localized concentrations of fine crystalline dolomite (Dol) within an aphanocrystalline/dolomicritic matrix (dMic). Visual porosity is poor within this sample. Scattered submicron pores were identified in association with the matrix (**see Figures 4.8-4.10**). **x119**

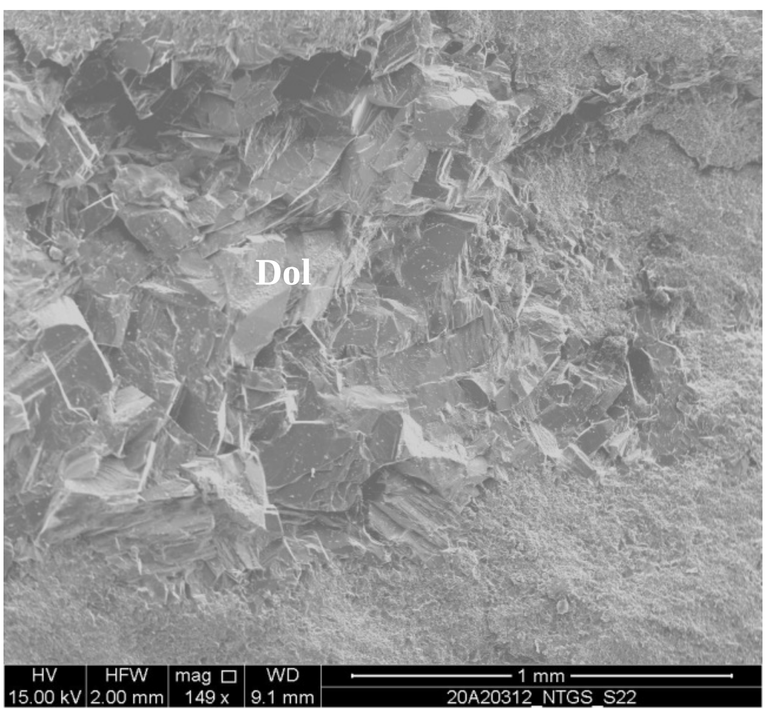


**SEM Figure 4.4. Sample S22, 10042.20ft/3060.86m.** Alternate low magnification view of fine crystalline replacement dolomite (Dol) which consists of tightly interlocking rhombs. Visual porosity is poor. **x149**

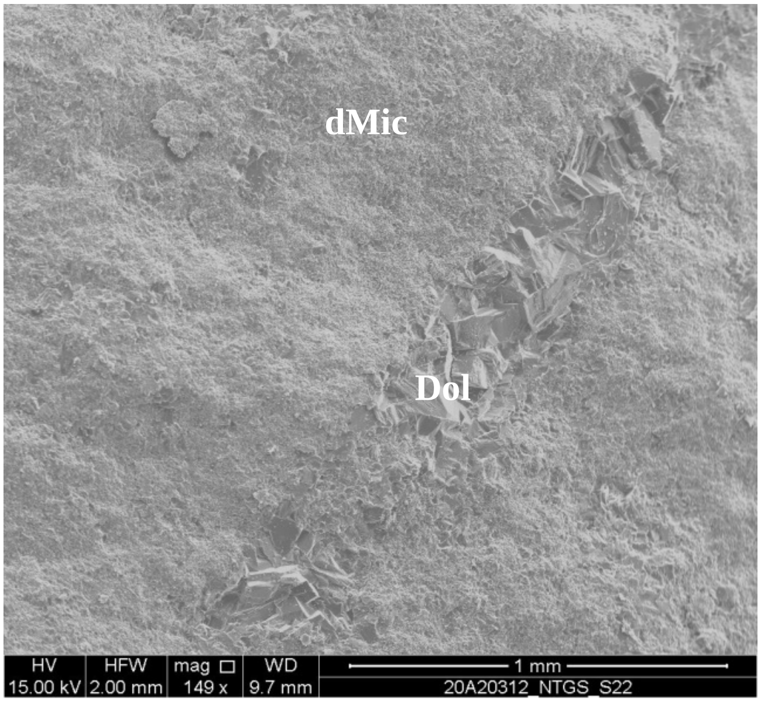


**SEM Figure 4.5. Sample S22, 10042.20ft/3060.86m.** Low magnification view of vein- or fracture-fill which consists of fine crystalline dolomite (Dol). Due to the tight interlocking fabric of the rhombic dolomite crystals, porosity is not well-preserved. dMic: dolomicrite/aphanocrystalline dolomite. **x149**

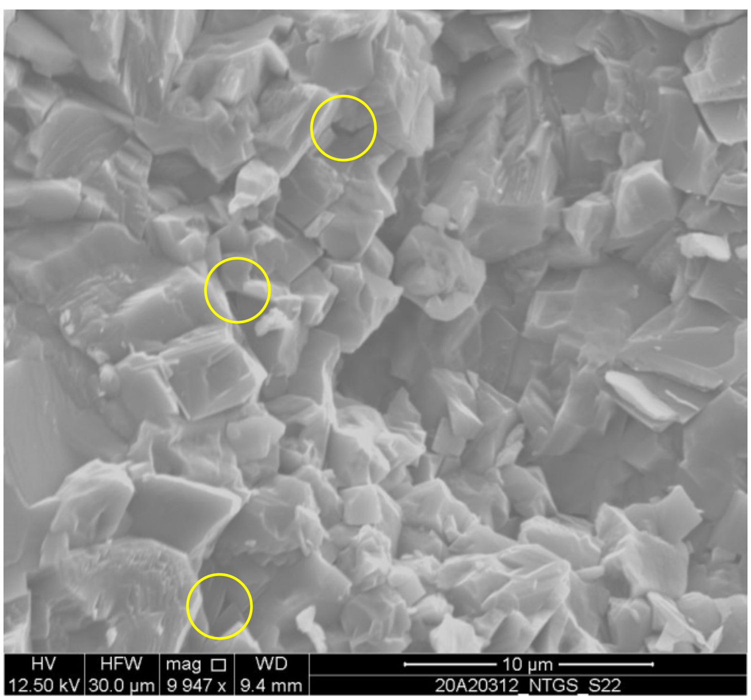


**SEM Figure 4.6. Sample S22, 10042.20ft/3060.86m.** High magnification image of the aphanocrystalline (<4µm) matrix. Scattered submicron pores are highlighted within this view. **x9947**

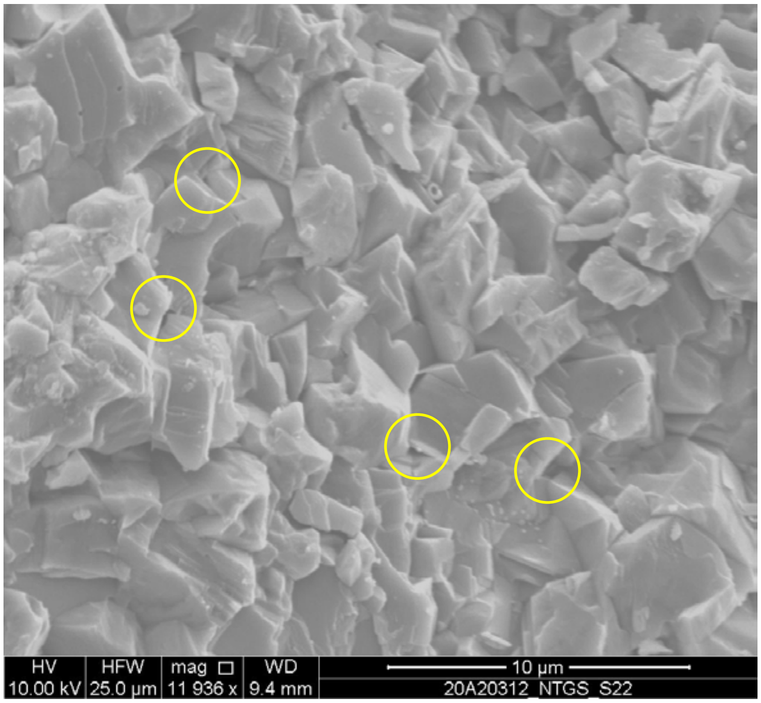


**SEM Figure 4.7. Sample S22, 10042.20ft/3060.86m.** Alternate high magnification view showing scattered submicron pore spaces within the dolomitic aphanocrystalline (<4µm) matrix. **x11936**

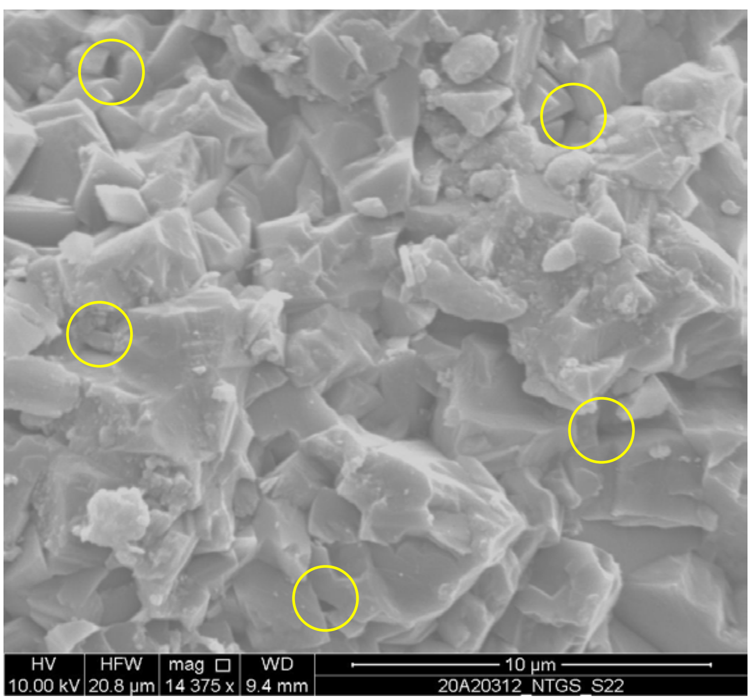


**SEM Figure 4.8. Sample S22, 10042.20ft/3060.86m.** Very high magnification alternate high magnification view showing scattered submicron pore spaces within the dolomitic aphanocrystalline (<4µm) matrix. **x14375**

## SUMMARY OF PORE SYSTEM, MAIN POROSITY CONTROLS AND RESERVOIR QUALITY

Porosity, permeability and overall reservoir quality of the dolostone at the study locations is a function of various controls that includes depositional controls of grain size, sorting and mineralogy, and the diagenetic controls of compaction (mechanical and chemical), dissolution and cementation. Dissolution porosity is (i.e. micro-vuggy) is rarely a true benefit to reservoirs since most of it is re-distributional porosity whereby the particles derived from the dissolved minerals are usually re-precipitated as cement elsewhere. For the dolostone samples, diagenesis, which is defined as chemical and physical alteration of sediments after deposition and prior to the onset metamorphism, is a primarily factor responsible for modification of original porosity.

Except for sample T24, which does not show any visible porosity, the other three samples have trace amounts of intercrystalline, micro-intercrystalline, micro-vuggy, and fracture pores. The main porosity reducing features observed in these samples is the abundance of micrite that plugged primary interparticle pores, plus the recrystallization of some of the micrite to tightly packed mosaic micro- and pseudospar. These samples also contain fair amount dolomite and calcite cement, which fills fractures, burrow walls, and replaces indistinct bioclast fragments.

Porosity as assessed by scanning electron microscope observation (SEM) is generally consistent with thin section observation. The pore system is characterized by scattered microporosity, often submicron pores, which occur in association with the micrite matrix. Porosity is absent where tightly interlocking crystal fabrics, which typically result from recrystallization, are dominant. Trace micro-intercrystalline ($\leq 5\mu m$) porosity noted in sample S23 is associated with probable bioclasts which have been replaced by rhombohedral dolomite cements.

Reservoir quality of these dolostone samples is mainly controlled by diagenesis (i.e. mineral diagenesis and compaction) and to lesser extent by depositional environment (i.e. crystal and grain size of the precursor carbonate rock, burrowing of the sediment, etc.). Reservoir quality is assessed as poor.

The following table summarizes the most important aspects that affected the reservoir quality of the four dolostone samples at the study location.

| Sample ID | Depth (ft/m) | Total Micrite (%) | Total Cement & Replacement (%) | Total Porosity (%) | | | | | Main Porosity controlling factors (*) | RQ (*) |
|---|---|---|---|---|---|---|---|---|---|---|
| | | | | IP | Ixl | mV | Fr | M | | |
| **Location: B.A. Texaco Arrowhead N-02 300/N-02-6040-12300/00** | | | | | | | | | | |
| T25 | 13137.00/4004.16 | 64 | 3 | - | TR | - | TR | - | Mic; Com; Cc; Dc; Py; Br; C | P |
| T24 | 13147.50/4007.36 | 25 | 11 | - | - | - | - | - | Mic; Com; Ms; Cc; Dc; Py; C | P |
| T23 | 13162.10/4011.81 | 45 | 3 | - | - | TR | TR | TR | Mic; Com; Dc; Cc; Py; C; Br | P |
| T22 | 13681.80/4170.21 | 38 | 6 | - | TR | - | - | - | Mic; Com; Ms; Cc; Dc; Py | P |

**Porosity value (%): IP** – interparticle porosity; **Int** – intraparticle; **Ixl** – intercrystalline; **Mv** – micro-vuggy; **Fr** – fracture porosity; **M** – micro-intercrystalline porosity
**Main Porosity controlling factors: Com –** compaction (mechanical and chemical)**; Dol** – dolomitization; M**ic** – micrite (calcite or dolomite) and/or micritization; **Ms** – micro- and/or pseudospar; **Cc** – calcite cement (druse and spar); **Dc** – dolomite cement**; C** – clays and organics; **Qc** – quartz/chert cement; **Ov** – crinoid overgrowths; P**y** – pyrite (replacement and/or cement); **OM** – organic matter/pyrobitumen; **Dis** – dissolution; **F** – fabric: [**CC** – concavo-convex orthochem contacts; **S** – sutured orthochem contacts]; **Br** - burrowing
**RQ (*) - reservoir quality: VP –** very poor; **P –** poor; **M –** moderate; **G –** good

**Total Micrite: Note that the Total Micrite column includes micrite and also micro- and pseudospar replacement of micrite.**

Reservoir problems for the samples recovered from the Nahanni Formation at the B.A. Texaco Arrowhead N-02 300/N-02-6040-12300/0 location, may include the following: **(1)** isolated and small sizes of intercrystalline, micro-intercrystalline, micro-vuggy and fracture pores, plus overall poor interconnectivity between pores could restrict the flow of hydrocarbons, **(2)** hydrochloric acid (HCl) treatment of this reservoir has the potential to loosen carbonate fines (dolo-micrite) that could migrate and block pore throats, plus cause fabric collapse, **(3)** the sensitivity of calcium carbonate to hydrofluoric acid (HF) in regard to precipitation of calcium fluoride scales.

In regards to overall poorly interconnected and heterogeneous pore system, fracture stimulation could be considered to create a more homogeneous production environment and to improve flow rates. After fracturing production rate should be held under a 'critical velocity' flow rate to avoid migration of formation fines created during fracturing.

## Comments in regards to the Routine Core Analysis vs Thin Section point counted porosity

Porosity and permeability results derived from the Routine Core Analysis (RCA) can be found in the Petrographic Summary Table 1. The information regarding routine porosity and permeability are presented only to compare different methods that could be used in the assessment of reservoir quality, plus to see what could possibly affect the results. The porosity and $K_{max}$ permeability that are listed in the Petrographic Summary Table 1 are of the routine core samples that were cut from the same interval as the thin section samples. The table below shows the thin section and RCA samples ID, spot depth that they represent, helium porosity ( Φ – %, and permeability ($K_{max}$), plus corresponding thin section sample point counting porosity.

| Sample ID | Depth (ft & m) | RCA results | | TS Porosity Φ(%) | Rock Classification |
|---|---|---|---|---|---|
| | | Φ (%) | $K_{max}$ (mD) | | |
| | | | | | |
| **Nahanni Formation** | | | | | |
| T25/P15 | 10015.50ft 3052.72m | 0.5 | 0.65* | TR | Dolostone (Mudstone) |
| T24/P14 | 10020.00ft 3054.10m | 1.4 | 0.12* | Nil | Dolostone (Packstone-Wackestone) |
| T23/P13 | 10023.75ft 3055.24m | 0.7 | 0.06* | TR | Dolostone (Mudstone-Wackestone-Packstone) |
| T22/P12 | 10042.20ft 3060.86m | 0.9 | 0.01* | TR | Dolostone (Wackestone-Packstone) |

**RCA – Routine Core Analysis; TS – Thin section (*) Permeability measurement affected by fractures**

Overall the thin section point counted porosity corresponds with the RCA results. All four samples are tight and it appears that even matrix (micrite) does not hold much of the porosity. Only small differences between both types of porosities is associated with carbonate fines, the heterogeneity of core and thin section samples (heterogeneous distribution of cements) and the difference in dimension (aspect ratio) of thin section and core samples[1]. It should be noted that the Routine Core Analyses measures both effective (visible) and non-effective porosity (microporosity), while the thin section petrology only point counts the visible pores.

[1] During the thin section examination a two-dimensional representative area is analyzed, whereas petrophysical core analysis reflects the three-dimensional pore volume.

## REFERENCES

Folk, R. L. (1974), Petrology of Sedimentary Rocks. Hemphills, Austin, Texas, USA.

Scholle, P.A. and Ulmer-Scholle, D.S. 2006. A Color Guide to the Petrography of Carbonate Rocks: Grains, Textures, Porosity, Diagenesis. AAPG Memoir 77. American Association of Petroleum Geologists, Tulsa, O.K.

Tucker, M. E. (1998). Sedimentary Petrology: An Introduction to the Origin of Sedimentary Rocks. Second Edition, Blackwell Science Ltd., Malden, Massachusetts.

Ulmer-Scholle, D.S., Scholle, P.A., Schieber, J. and Raine, R.J. 2014. A Color Guide to the Petrography of Sandstones, Siltstones, Shales and Associated Rocks. AAPG Memoir 109. American Association of Petroleum Geologists, Tulsa, O.K.

Welton, J.E. 2003. SEM Petrology Atlas. Methods in Exploration Series No. 4. American Association of Petroleum Geologists, Tulsa, O.K.

# DATA TABLES

# TABLE 1
## Petrographic Summary of Four Samples from the Nahanni Formation at the B.A. Texaco Arrowhead N-02 300/N-02-6040-12300/0 Location

| | | | | | | | |
|---|---|---|---|---|---|---|---|
| **Sample ID** | | **T25** | **T24** | **T23** | **T22** | | |
| **Depth (ft)** | | **10015.50** | **10020.00** | **10023.75** | **10042.20** | | |
| **Rock Type** | | **Dol** | **Dol** | **Dol** | **Dol** | | |
| **Mineralogy** | *Calcite* | 1 | 5 | 1 | 4 | | |
| | *Dolomite* | 68 | 94 | 84 | 96 | | |
| | *Anhydrite* | - | - | - | - | | |
| | *Quartz/Chert* | 30 | - | 15 | . | | |
| | *Feldspar* | - | - | - | - | | |
| | *Rock Fragments* | TR | - | - | - | | |
| | *Pyrite and Heavy Minerals* | 1 | 1 | TR | TR | | |
| | *Phosphate* | - | - | - | - | | |
| | *Clays & organics* | TR | TR | TR | TR | | |
| **Total Rock Volume (%)** | | **100** | **100** | **100** | **100** | | |
| **Carbonate Clasts** | *Peloids* | 1 | 20 | 35 | 30 | | |
| | *Ooids/Oolites* | TR | - | TR | - | | |
| | *Intraclasts/Onocolites* | 2 | - | TR | 1 | | |
| | ***Total:*** | **3** | **20** | **35** | **31** | | |
| **Bioclasts/Fauna** | *Mollusks* | - | 4 | | 10 | | |
| | *Foraminifers* | - | - | - | - | | |
| | *Brachiopod (shell & spines)* | - | 10 | | | | |
| | *Bryozoans* | - | - | - | - | | |
| | *Corals* | - | - | 1 | | | |
| | *Algae* | - | - | - | 5 | | |
| | *Echinoderms/Crinoids* | - | - | - | | | |
| | *Ostracodes* | - | TR | TR | 5 | | |
| | *Annelid worms* | - | 25 | - | - | | |
| | *Unidentified* | - | 5 | 1 | 5 | | |
| | ***Total:*** | **0** | **44** | **2** | **25** | | |
| **Detrital Grains** | *Quartz/Chert* | 30 | - | 15 | - | | |
| | *Feldspar* | - | - | - | - | | |
| | *Rock Fragments* | TR | - | - | - | | |
| | *Heavy minerals* | - | - | - | - | | |
| | ***Total:*** | **30** | **0** | **15** | **0** | | |
| **Matrix** | *Micrite (calcite or dolomite)* | 64 | 15 | 45 | 19 | | |
| | *Micro- and pseudospar* | - | 10 | - | 19 | | |
| | *Clay and Organics* | TR | TR | TR | TR | | |
| | *Sutured Allochems* | - | - | - | - | | |
| | ***Total:*** | **64** | **25** | **45** | **38** | | |
| **Pore Filling Cement** | *Calcite Spar* | 1 | 5 | 1 | 2 | | |
| | *Calcite Druse* | - | - | - | 2 | | |
| | *Dolomite* | 1 | 5 | 2 | 2 | | |
| | *Ferroan Dolomite* | - | - | - | - | | |
| | *Quartz Overgrowths* | - | - | - | - | | |
| | *Pyrite* | - | 1 | - | - | | |
| | *Anhydrite* | - | - | - | - | | |
| | ***Total:*** | **2** | **11** | **3** | **6** | | |
| **Replacement** | *Calcite* | - | - | - | - | | |
| | *Dolomite* | - | - | - | - | | |
| | *Anhydrite* | - | - | - | - | | |
| | *Quartz/Chert* | - | - | - | - | | |
| | *Pyrite* | 1 | TR | TR | TR | | |
| | ***Total:*** | **1** | **TR** | **TR** | **TR** | | |
| **Total Rock Volume (%)** | | **100** | **100** | **100** | **100** | | |
| **Crystal Texture (Matrix)** | | Anh | Anh | Anh | Anh | | |
| **Crystal Texture (Cement)** | | Euh | Sub-Euh | Sub-Euh | Sub-Euh | | |
| **Cristal size (Dolomite)** | | Aph | Aph | Aph | Aph | | |
| **Structure** | | Fracs; Lm; Br | Fracs | Br; Fracs;Styl | Lm; Fracs; GP | | |
| **Fabric** | | - | - | - | - | | |
| **Ratio Matrix/Clasts (approximate)** | | 20:1 | 1:2 | 2:1 | 1:2 | | |
| **Original Texture** | | MS | PS-WS | MS-WS-PS | WS-PS | | |
| **Porosity** | *Interparticle* | - | - | - | - | | |
| | *Intraparticle* | - | - | - | - | | |
| | *Intercrystalline* | TR | - | - | TR | | |
| | *Biomoldic* | - | - | - | - | | |
| | *Micro-Vuggy* | - | - | TR | - | | |
| | *Fractures* | TR | - | TR | - | | |
| | *Micro-Intrecrystalline pores* | - | - | TR | - | | |
| | ***Total TS Porosity (%)*** | **TR** | **0** | **TR** | **TR** | | |
| **Petrophysical Results** | *Core Porosity (%)* | **0.50** | **1.40** | **0.70** | **0.90** | | |
| | *Gas Permeability (mD)* | **0.65*** | **0.12*** | **0.06*** | **0.01*** | | |
| **Reservoir Quality** | | **Poor** | **Poor** | **Poor** | **Poor** | | |

# LIST OF ABBREVIATIONS (CARBONATES)

## SKELETAL GRAINS

| | | |
|---|---|---|
| Bry | - | BRYOZOAN |
| Ech | - | ECHINODERMS |
| Bra | - | BRACHIOPODS |
| Os | - | OSTRACODS |
| Cal | - | CALCISPHERES |
| Moll | - | MOLLUSKS |
| Plcy | - | PELECYPODS |
| Biv | - | BIVALVES |
| For | - | FORAMINIFERA |
| Strom | - | STROMATOPOROIDS |
| Cor | - | CORALS |
| Ga | - | GASTROPODS |
| Biocl | - | BIOCLASTS |

## OTHER GRAINS

| | | |
|---|---|---|
| Pel | - | PELOIDS |
| Ooi | - | OOIDS |

## ORIGINAL TEXTURE

| | | |
|---|---|---|
| GS | - | GRAINSTONE |
| PS | - | PACKSTONE |
| WS | - | WACKESTONE |
| MS | - | MUDSTONE |
| FS | - | FLOATSTONE |
| RS | - | RUDSTONE |

## CRYSTAL TEXTURE

| | | |
|---|---|---|
| Euh | - | EUHEDRAL |
| Sub | - | SUBHEDRAL |
| Anh | - | ANHEDRAL |

## CRYSTAL SIZE

| | | |
|---|---|---|
| Cxl | - | COARSE CRYSTALLINE |
| Mxl | - | MEDIUM CRYSTALLINE |
| Fxl | - | FINE CRYSTALLINE |
| Vfxl | - | VERY FINE CRYSTALLINE |

## CEMENT TYPES

| | | |
|---|---|---|
| Syn | - | SYNTAXIAL OVERGROWTHS |
| Blo | - | BLOCKY |
| Poik | - | POIKILOTOPIC |
| Dru | - | DRUSY |
| SD | - | SADDLE DOLOMITE |
| Lath | - | ANHYDRITE LATHS |
| Grm | - | GROUNDMASS |
| Iso | - | ISOPACHOUS RIMS |
| Spa | - | SPARITE |

## POROSITY TYPES

| | | |
|---|---|---|
| Mixl | - | MICRO-INTERCRYSTALLINE |
| Ixl | - | INTERCRYSTALLINE |
| Mo | - | BIOMOLDIC |
| mV | - | MICROVUGGY |
| mF | - | MICROFRACTURE |
| IG | - | INTERGRANULAR |
| IP | - | INTERPARTICLE |
| INTRP | - | INTRAPARTICLE |

## QUALITY

| | | |
|---|---|---|
| G | - | GOOD |
| M | - | MODERATE |
| P | - | POOR |

**Well Name:** B.A. Texaco Arrowhead N-02
**Well ID:** 300/N-02-6040-12300/0
**NT WID #** N240

**Table 2**: Results of quantitative mineral analysis (relative weight %) of X-ray diffraction data for 4 (four) samples using Rietveld method

| Geology ID | Depth (ft) | Depth (m) | Core & Box # | NTGS Sample Type & # | **Calcite** | **Dolomite** | **Quartz** | **Plagioclase feldspar** | **Muscovite/ Illite** | **Pyrite** | **Total** |
|---|---|---|---|---|---|---|---|---|---|---|---|
| 1 | 10015.50 | 3052.72 | 5 & 1 of 7 R | T25, X43, S25, P15 | 0.4 | 93.4 | 2.8 | 0.8 | 2.4 | 0.2 | 100 |
| 2 | 10020.00 | 3054.10 | 5 & 2 of 7 R | T24, X42, S24, P14 | | 98.9 | 0.3 | 0.8 | | | 100 |
| 3 | 10023.75 | 3055.24 | 5 & 3 of 7 R | T23, X41, S23, P13 | | 95.6 | 3.5 | 0.5 | 0.3 | 0.1 | 100 |
| 4 | 10042.20 | 3060.86 | 5 & 6 of 7 L | T22, X40, S22, P12 | | 99.4 | 0.1 | 0.5 | | | 100 |

AGAT Laboratories